RSC Advances

PAPER

View Article Online
View Journal | View Issue

Cite this: *RSC Adv.*, 2025, **15**, 7050

Catalytic solid derived from residual bean husk biomass applied to sustainable biodiesel production: preparation, characterization, and regeneration study

Izadora de Araújo Sobrinho, Thaíssa Saraiva Ribeiro, Ane Caroline Dias e Silva, Matheus Arrais Gonçalves, Geraldo Narciso da Rocha Filho and Leyvison Rafael Vieira da Conceição *

This study investigates the use of bean husks as a precursor for the synthesis of an efficient and regenerable catalyst, with the aim of offering an economical and sustainable alternative for biodiesel production. Residual bean shell biomass (RBBH) was calcined at different temperatures (350–500 °C) and times (1–4 h) to determine the optimum synthesis conditions. The catalyst obtained was characterized by various methods, such as X-ray Diffraction (XRD), Fourier Transform Infrared Spectroscopy (FT-IR), Scanning Electron Microscopy (SEM), Energy Dispersive X-ray Spectroscopy (EDS) and Thermogravimetric Analysis (TG/DTG). The results showed that the catalyst contains metal oxides and carbonates as active sites. In addition, the influence of reaction conditions was evaluated in the ranges of temperature (60–120 °C), time (0.5–2.5 h), MeOH : oil molar ratio (12 : 1–28 : 1) and catalyst concentration (2–10% by weight). The maximum ester content (97.6%) was achieved at 120 °C, 2 h, a MeOH : oil molar ratio of 20 : 1 and 8% catalyst. After partial deactivation of the solid catalyst, it was regenerated with KOH, yielding biodiesels with an ester content of over 75% in three consecutive cycles, demonstrating its efficiency and potential for continuous use.

Received 18th February 2025
Accepted 25th February 2025

DOI: 10.1039/d5ra01195g

rsc.li/rsc-advances

1. Introduction

Fossil fuels have a high energy production capacity and calorific value and have been widely used since the advent of the Industrial Revolution, becoming the world's primary energy source.[1] However, the combustion of fossil fuels causes environmental damage and poses health risks due to the emission of particulate matter, pollutants, and toxic gases. Additionally, the growing energy consumption compromises the availability of these resources, as they are derived from non-renewable sources.[2] Thus, biofuels present a viable alternative energy source, playing a significant role in addressing these challenges with a range of environmental, economic, and social advantages. Among them, biodiesel holds the greatest potential as a substitute for petroleum derivatives due to its physical properties, which are similar to those of diesel fuel.[3]

Biodiesel is chemically defined as a mixture of alkyl esters of fatty acids, which can be obtained through esterification or transesterification. In these processes, fatty acids or triglycerides derived from vegetable oil or animal fat react with primary alcohols (methanol or ethanol), forming the respective products.[4] These reactions are reversible, so an excess of alcohol is required to favor product formation. Additionally, the reactions can occur through basic, acidic, or enzymatic catalysis. Currently, homogeneous catalysts are used in the industrial production of biodiesel. Although homogeneous catalysts exhibit good catalytic activity, they have several environmental and economic limitations, such as issues with effluents generated during product purification, and they are neither recoverable nor reusable.[5,6] Consequently, the costs associated with biodiesel production are high.

In contrast, heterogeneous catalysis has gained more attention due to its properties, such as high catalytic activity, selectivity, and, most importantly, ease of separation from the reaction medium, reusability, and regenerability.[7] Some of these heterogeneous catalysts can be derived from residual biomasses that are typically discarded without any application. This highlights the availability of raw materials and, consequently, the processing costs of biodiesel can be reduced.[6] The literature reports several studies on the synthesis of heterogeneous catalysts from biomasses, such as orange peels,[8] açaí seeds,[9] cupuaçu seeds,[10] banana peels,[11] rice husks,[12] coconut shells,[13] among others.

Federal University of Pará, Institute of Exact and Natural Sciences, Graduate in Chemistry Program, Laboratory of Catalysis and Oleochemical, 66075-110, Belém, Pará, Brazil. E-mail: rafaelvieira@ufpa.br

Some studies report the easy processing of certain biomasses, which, when subjected to thermal treatment, exhibit catalytic potential without requiring additional steps. For example, in studies conducted by Daimary *et al.*[14] and Laskar *et al.*,[15] potato peels and mango (*Mangifera*) peels were used as precursors in the synthesis of a basic heterogeneous catalyst applied to biodiesel production. The authors reported that, after thermal treatment, the biomasses demonstrated catalytic potential, achieving maximum ester content of 97.5% and 98%, respectively. These high ester contents are attributed to the components of the catalyst, such as alkali metal oxides and carbonates (K, Ca, Mg, Na), with potassium being predominant in the composition of both catalysts. These formed compounds characterize the alkalinity of the synthesized catalyst.

The catalyst employed in successive transesterification cycles for biodiesel production may exhibit a reduction in ester content due to catalytic deactivation, indicating potential leaching of active sites into the reaction medium, pore blockage due to the deposition of triglycerides and glycerol on the catalyst surface, and/or mass loss of the catalyst during the recovery and purification stages.[16] Consequently, the number of available active sites is limited, reducing the interactions between the catalyst and the liquid phases, which results in lower ester content. A mechanism for recovering catalytic properties is the application of the regeneration method, which aims to increase the number of active sites on the catalyst surface.

In Brazil, there is a wide variety of beans that are a staple in the Brazilian diet. Among them is *Vigna unguiculata* L. Walp., commonly known as cowpea beans, which is the second most produced type of bean in the country. According to data from IBRAFE (Brazilian Institute of Beans and Pulses), it is estimated that in 2022, Brazil produced approximately 629.3 thousand tons of cowpea beans.[17] This highlights the generation of large quantities of agro-industrial waste. The reuse of waste produced by human activities is still limited; however, lignocellulosic residues show potential for specific applications,[18] as demonstrated by studies using bean husks as adsorbents for organic dyes,[19] pharmaceuticals,[20] and as a source of cellulose.[18]

Given the limited applications mentioned above, developing value-added products is crucial for sustainable development. Therefore, this study proposes the synthesis of a basic heterogeneous catalyst derived from bean husks, a low-cost, widely available, and easily processed precursor, with the aim of obtaining an efficient catalyst for biodiesel production.

2. Materials and methods

2.1. Materials

The residual biomass of bean husks (RBBH) used in this study was collected from family farms in the Metropolitan Region of Belém, Pará, Brazil. Refined soybean oil was purchased from a local market. Methyl alcohol (CH_3OH, 99.8%), heptane (C_7H_{16}, 99.5%), and potassium hydroxide (KOH, 97%) were acquired from Dinâmica. Hexane (C_6H_{14}) and sodium hydroxide (NaOH, 97%) were purchased from Neon, while hydrochloric acid (HCl, 37%) was obtained from Isofar. The chromatographic standard methyl heptadecanoate ($C_{18}H_{36}O_2$, 99%) was purchased from Sigma-Aldrich. It is worth noting that all reagents used were of analytical grade.

2.2. Catalyst preparation

The catalyst was synthesized through a thermal treatment process, responsible for the carbonization of organic residues, resulting in an ash-rich material. The methodology used was described by Aleman-Ramirez *et al.*[21] with slight modifications. Initially, the RBBH was collected, dried, and ground in a Quimis analytical mill until a fine powder of approximately 70 mesh was obtained. In a typical procedure, 25 g of RBBH powder was thermally treated in a muffle furnace, with the calcination temperature and time varying between 350 °C to 500 °C and 1 h to 4 h, respectively, using a heating rate of 10 °C min^{-1}. The selection of these calcination temperature and time ranges was based on preliminary tests, which helped define an appropriate interval for the study, in addition to values reported in the literature for similar materials.[13,14] After this step, the material obtained was cooled to room temperature, ground, weighed, and stored in a desiccator to avoid contact with atmospheric air. The catalysts were designated as BHA*T*/*t*, where BHA stands for bean husk ash, and *T* and *t* represent calcination temperature and time, respectively.

2.3. Material characterization

The determination of basic groups present in the catalysts was performed by acid–base titration according to the method described by Boehm *et al.*[22] with adaptations. In this method, 0.25 g of the sample was weighed into a beaker, and 30 mL of 0.1 mol per L HCl solution was added. The mixture was then stirred magnetically for 24 h at room temperature. At the end of this period, the mixture was centrifuged, and a 10 mL aliquot of the filtrate was mixed with 15 mL of a 0.10 mol per L NaOH standard solution. The excess NaOH was then titrated with 0.10 mol per L HCl solution, using phenolphthalein as an indicator. X-ray diffraction (XRD) patterns of the BHA400/3 and BHA400/3-R catalysts were determined using a Bruker D2 PHASER diffractometer, applying the powder method. The radiation used was Cu Kα (1.54 Å), with a voltage of 40 kV and current of 40 mA, and a scanning range of $10° < 2\theta > 65°$. Fourier Transform Infrared Spectroscopy (FT-IR) analyses were performed using a Shimadzu IR Prestige-21 spectrometer. The samples were pressed into KBr, and the spectra were collected in the range of 3600–400 cm^{-1} with a resolution of 4 cm^{-1} and a total of 32 accumulations. The surface morphologies of the materials were recorded by Scanning Electron Microscopy (SEM), using a Tescan VEGA 3 LMU microscope operating at an acceleration voltage of 20 kV. Surface elemental mappings were performed by Energy Dispersive X-ray Spectroscopy (EDS), using an Oxford AZtec Energy X-Act microanalysis system with a resolution of 129 eV. The Thermogravimetric Analyses (TG/DTG) of RBBH and the BHA400/3 catalyst were performed using a Shimadzu DTG-60H instrument over a temperature range of 25 °C to 700 °C, with a heating rate of 10 °C min^{-1}, under a nitrogen atmosphere (flow rate of 50 mL min^{-1}), and in an alumina crucible.

2.4. Biodiesel production

The transesterification reaction of soybean oil with methanol was conducted in a PARR 5500 HPCL Compact Reactor. The reactions occurred in a pressurized system, with temperature control and fixed stirring at 700 rpm. During this process, the influence of reaction conditions on the ester content of the produced biodiesel was evaluated, varying the reaction temperature (60–120 °C), reaction time (0.5–2.5 h), molar ratio MeOH : oil (12 : 1–28 : 1), and catalyst concentration (2–10 wt%). Upon completion of the reaction, the products were separated from the catalyst by centrifugation, and then the phase containing the methyl esters was washed with distilled water at 80 °C to remove residual methanol and glycerol. Subsequently, the residual water present in the biodiesel was removed by drying in an oven at 60 °C for 12 h. Finally, the synthesized biodiesel was stored under refrigeration for ester content determination analysis.

2.5. Biodiesel characterization

2.5.1. Ester content determination. The synthesized biodiesels were characterized by gas chromatography using the methodology adapted from the European standard EN 14103 as proposed by Silva *et al.*[23] Therefore, the ester content was determined using heptane as the solvent and methyl heptadecanoate as the chromatographic standard in a Varian CP 3800 gas chromatograph (GC) equipped with a flame ionization detector (FID), a CP WAX 52 CB capillary column 30 m long with 0.32 mm diameter, and a 0.25 μm film. Helium gas was used as the mobile phase with a flow rate of 1 mL min^{-1} and an injection volume of 1 μL. The initial oven temperature was programmed to 170 °C, with a heating rate of 10 °C min^{-1}, until reaching the final temperature of 250 °C (the same temperature as the FID and injector). The ester content was calculated using eqn (1) below:

$$\text{Ester content (\%)}: \frac{(\sum A_T) - A_{IS}}{A_{IS}} \times \frac{C_{IS}}{C_{B100}} \times 100 \qquad (1)$$

where: $\sum A_T$ corresponds to the sum of the total areas of the peaks; A_{IS} is the peak area of the internal standard; C_{IS} is the concentration of the internal standard solution; and C_{B100} is the concentration of biodiesel after dilution.

2.5.2. Physicochemical properties of biodiesel. The quality of the produced biodiesel was determined through physicochemical analyses established by the American Society for Testing and Materials (ASTM) to assess its applicability in engines. The kinematic viscosity at 40 °C was determined according to ASTM D445, using a Cannon-Fenske viscometer (SCHOTT GERATE, 520 23). Density was measured at a temperature of 20 °C according to ASTM D6890, with an automatic densimeter KEM DAS-500. The acid value of the biodiesel was determined according to ASTM D664. The cold filter plugging point was determined according to ASTM D6371 using a TANAKA AFP-102 apparatus. The flash point was determined according to ASTM D93 using a TANAKA APM 7 Pensky-Martens automatic apparatus. Finally, copper corrosion was determined according to ASTM D130 in a Koehler corrosion bath.

2.6. Recovery and regeneration of the BHA400/3 catalyst

After the first transesterification reaction, the catalyst was recovered by centrifugation at 2000 rpm for 10 min, followed by washing with two portions of ethyl alcohol (15 mL) and one portion of hexane (10 mL) to remove residual mono-, di-, and triglycerides, as well as unreacted glycerol. The catalyst was then dried in an oven at 100 °C for 12 h. Subsequently, the catalyst was reused in the transesterification reaction under optimized reaction conditions.

However, when a reduction in the ester content of the synthesized biodiesel was observed after the reaction cycle, an additional regeneration step was performed on the BHA400/3 catalyst using the wet impregnation method described by Foroutan *et al.*[24] with adaptations. The catalyst was doped with different K concentrations ranging from 5.0, 10.0 and 15.0 wt%, using a solid-to-liquid ratio of 1 g to 20 mL of KOH solution, under magnetic stirring at 60 °C for 1 h. The catalyst was then dried in an oven at 100 °C for 24 h and calcined at temperatures of 200 °C, 300 °C, and 400 °C for 3 h. The KOH was used as a doping agent because potassium is the predominant element in the catalyst composition, which accounts for its high basicity. The regenerated catalyst was denoted as BHA400/3-R, where BHA refers to the bean husk ash synthesized by thermal treatment at 400 °C for 3 h, and R stands for regenerated.

3. Results and discussion

3.1. Evaluation of the influence of catalyst synthesis conditions on the ester content of the produced biodiesel

3.1.1. Influence of calcination temperature on catalyst performance. The synthesis conditions of the catalyst, such as the temperature and calcination time of the residual biomass of bean husks (RBBH), influence the concentrations of certain species present in the ashes and carbonaceous compounds formed during the catalyst production process, which directly impacts the catalytic performance in biodiesel production. Thus, the RBBH was carbonized at a temperature range of 350 °C to 500 °C and time ranging from 1 h to 4 h, and the produced catalysts were employed in catalytic tests conducted under non-optimized reaction conditions: temperature of 120 °C, time of 2 h, molar ratio MeOH : oil of 24 : 1, and catalyst concentration of 10 wt%.

Fig. 1 shows the influence of varying the calcination temperature of RBBH on the synthesis of the catalysts, the ester contents of the biodiesels produced with the respective catalysts, and the basicity for each tested catalyst. It is important to note that in this synthesis stage, the calcination time was fixed at 3 h. Based on the presented results, it is possible to observe that the catalysts synthesized at calcination temperatures of 350 °C, 400 °C, and 450 °C showed ester contents above 80%. However, the catalyst synthesized at 400 °C stood out, producing biodiesel with an ester content of 95.6% ± 0.51.

The presented results show that RBBH calcined at these temperatures promotes incomplete carbonization, resulting in significant amounts of carbonaceous species from the degradation of the main organic components, such as hemicellulose,

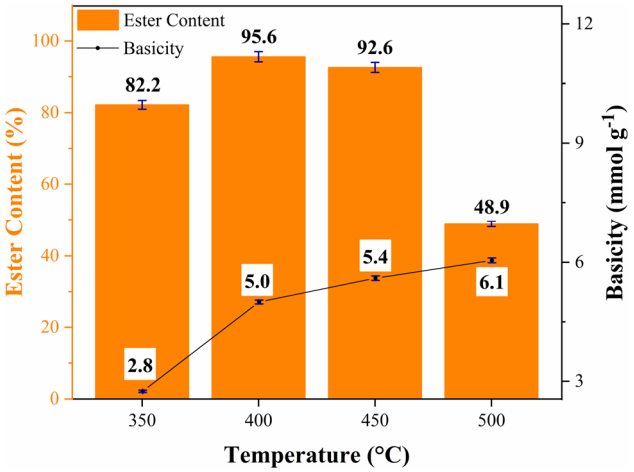

Fig. 1 Evaluation of the influence of calcination temperature on catalytic activity for biodiesel production and the basicity of synthesized catalysts.

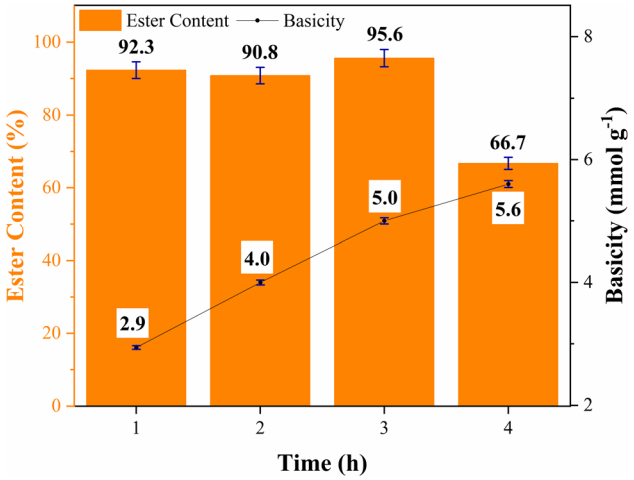

Fig. 2 Evaluation of the influence of calcination time on catalytic activity for biodiesel production and the basicity of synthesized catalysts.

cellulose, and lignin.[25] However, when the catalyst synthesized at 500 °C was used in the transesterification reaction, it resulted in biodiesel with an ester content of 48.9% ± 0.19. This represents a decrease of approximately 50% in catalytic activity compared to the ester content of biodiesel synthesized with the catalyst calcined at 400 °C (95.6% ± 0.51). Therefore, it is clear that using a calcination temperature of 500 °C favors the reduction of carbonaceous species in the catalyst, suggesting that as the amount of carbonaceous species decreases, there is less dispersion of the active phases (metal oxides and carbonates) in the catalyst, leading to a decrease in catalytic activity.[26]

These observations can be confirmed by the results obtained from the basicity analysis of the synthesized catalysts, shown in Fig. 1. In general, it is observed that as the calcination temperature increases, catalysts with higher basicity values are obtained. However, although the basicity of the materials is high, this alone does not guarantee that using the catalysts will result in biodiesels with high ester contents, as other factors determine catalytic activity, such as surface area and active phase distribution during catalyst formation,[27] since the catalytic process is a surface phenomenon.[28] This explains why using a calcination temperature of 500 °C results in a catalyst with the highest basicity (6.1 mmol g^{-1} ± 0.06) among the studied catalysts but produces biodiesel with an ester content of only 48.9% ± 0.19.

Therefore, the calcination temperature of 400 °C was selected to continue the evaluation of the influence of catalyst synthesis time on biodiesel production, as the catalyst obtained at this temperature produced biodiesel with a high ester content (95.6% ± 0.51), and the determined basicity value represents a good formation and homogeneity between metal oxides and carbonates (active sites) and carbonaceous species (inert part), meaning better dispersion of the active sites on the inert part of the catalyst.

3.1.2. Influence of catalyst calcination time. Fig. 2 shows the influence of varying the calcination time of RBBH in catalyst synthesis, as well as the ester content of the biodiesels produced using the respective catalysts and their basicity results. It is important to highlight that in these syntheses, the calcination temperature was kept constant at 400 °C.

The catalysts synthesized with calcination times of 1, 2 and 3 h, when applied in the transesterification reaction, resulted in biodiesels with high ester content of 92.3% ± 0.47, 90.8% ± 0.43, and 95.6% ± 0.51, respectively. The data suggest that synthesis times between 1 h and 3 h are sufficient to promote the incomplete carbonization of RBBH, resulting in significant amounts of carbonaceous compounds and a good formation of oxides and metallic carbonates in their constitution, making these catalysts efficient in biodiesel production. However, the catalyst calcined for 4 h showed a reduction in catalytic performance, yielding a biodiesel ester content of 66.7% ± 0.26, representing an average decrease of 26.2% in ester content compared to the biodiesel produced by the catalysts calcined for 1 h, 2 h, and 3 h.

These results indicate that calcination times of 4 h or longer used in catalyst synthesis lead to decreased catalyst activity, thereby limiting the maximization of methyl ester content in the transesterification reaction. This may be related to the fact that a greater amount of carbonaceous species is degraded during the process, leading to a significant reduction in surface area and poor dispersion of the active phases on the catalyst surface, which consequently reduces the interaction area between basic sites and the reactants. This behavior was also observed in studies conducted by Avhad and Marchetti[29] and Dejean *et al.*[30] on biomass used as precursor catalysts for biodiesel synthesis.

Moreover, these observations are supported by the basicity results obtained for the synthesized catalysts, as the gradual increase in time affects the material's composition and, consequently, its catalytic activities and properties.[30] As shown in Fig. 2, as the calcination time increases, the basicity of the catalysts also increases due to the higher concentration of oxides and metallic carbonates formed during thermal treatment. However, this did not result in an increase in ester

content in the biodiesel, as other factors influence catalytic activity, as mentioned earlier.[28]

On the other hand, the opposite behavior is observed when the catalyst was synthesized at 1 h and 2 h, where shorter times resulted in high ester contents but lower basicities. This is attributed to the lower concentration of oxides and carbonates in the catalyst, as the 1 h time is not sufficient to degrade the organic material, meaning there is a significant amount of carbonaceous species present.[31,32] However, the lower amount of active sites did not compromise the ester content of triglycerides to methyl esters during the transesterification reaction, possibly due to the formation of the surface area and the dispersion of the active phases in the catalyst, which is one of the key factors for efficient catalysis.[33]

However, the 3 h time resulted in the highest ester content to biodiesel of 95.6% ± 0.51. Additionally, the catalyst synthesized in this time showed a significant basicity value compared to the catalysts calcined at 1 h and 2 h, and slightly lower than the catalyst synthesized at 4 h. The high ester content and basicity indicate that the 3 h time was sufficient to improve catalytic performance. Therefore, a temperature of 400 °C and a time of 3 h were determined to be the best conditions for catalyst synthesis, in this case referred to as BHA400/3.

3.2. Characterization of RBBH and the BHA400/3 catalyst

The crystalline components present in the BHA400/3 catalyst were identified by XRD, and the diffraction pattern is shown in Fig. 3(a). The peak of highest intensity observed in the spectrum at $2\theta = 28.8°$ corresponds to the presence of K_2CO_3. Additionally, three other peaks related to this crystalline phase are located at $2\theta = 28.05°$, 33.9°, and 41.8°. The presence of K_2O is confirmed by peaks observed at $2\theta = 13.27°$, 39.39°, 40.5°, 47.49°, and 62.33°. The peaks corresponding to the phases identified as K_2CO_3 and K_2O are also reported in studies by Basumatary *et al.*,[34] Chutia *et al.*,[35] Khiangte *et al.*,[36] and Nath *et al.*,[37] who synthesized basic heterogeneous catalysts from residual biomass such as *Musa champa* peels, *Xanthium strumarium* seeds, dragon fruit peel, and *Sesamum indicum* plant residues, respectively.

The peaks found at $2\theta = 19.43°$, 29.34°, 30.41°, and 44.5° indicate the presence of Ca in different forms, such as hydroxide (19.43°), carbonate (29.34°), and oxide (30.41° and 44.5°). Similar values have been reported in the literature by Miladinović *et al.*,[38] Khiangte *et al.*,[36] Chutia and Phukan,[39] and Nath *et al.*[37] Meanwhile, the peaks at values of 42.9° and 48.36° correspond to MgO present in the catalyst, with similar values also reported in the studies by Miladinović *et al.*[38] and Eldiehy *et al.*[40] The peak at $2\theta = 33.3°$ is attributed to the Na_2O phase, which is also reported in the study conducted by Nath *et al.*[37] These identified functional groups, which are widely reported in the literature, play a crucial role in catalytic activity. The carbonate and metal oxide species act as basic active sites, facilitating the transesterification reaction and improving the efficiency of biodiesel production. Therefore, the XRD pattern confirms that the catalytic activity of the BHA400/3 catalyst is associated with the presence of alkali metals in the forms of oxides and carbonates, with potassium being the major component.

The FT-IR spectrum of the BHA400/3 catalyst is illustrated in Fig. 3(b) and shows different absorption bands and intensities in the studied wavelength range. The absorption bands at 2910 cm^{-1} and 2325 cm^{-1} are attributed to the stretching vibrations of C–H and M–O–K bonds (M: Si, Mg, Ca, *etc.*).[9,41] The intense band observed in the spectrum at 1444 cm^{-1} corresponds to the stretching and bending vibrations of C–O carbonate formed by the adsorption of atmospheric CO_2, which reacted with alkaline metal oxides present on the catalyst's surface during its synthesis.[15] Meanwhile, the band at 868 cm^{-1} is related to the in-plane and out-of-plane angular deformation vibrational modes of the carbonate group (CO_3^{2-}), suggesting the presence of metal carbonates such as K_2CO_3 and Ca_2CO_3.[42]

The vibrational band at 1058 cm^{-1} can be attributed to the symmetric stretching of C–O due to the breakdown and depolymerization of lignin, cellulose, and hemicellulose.[41] Additionally, the absorption bands identified in the spectrum at

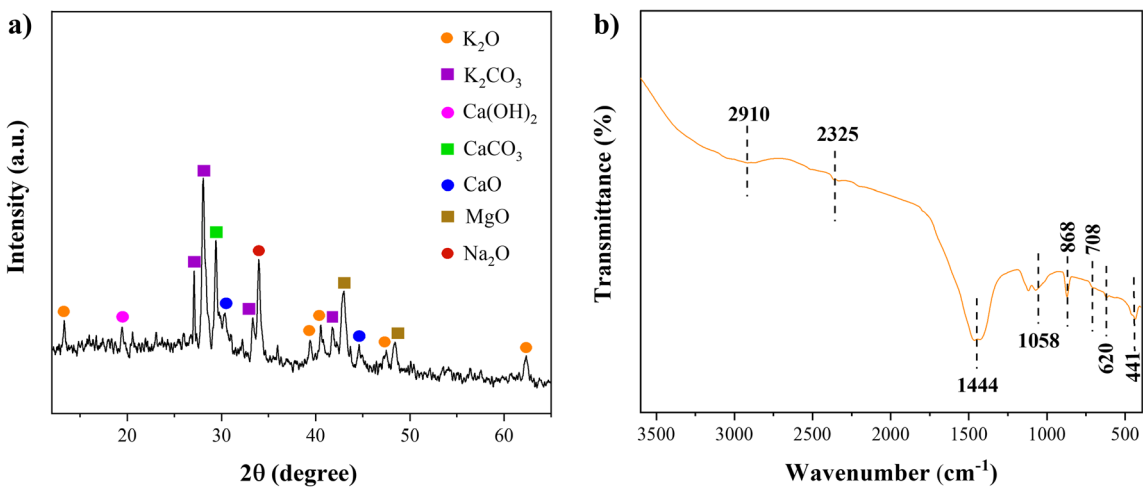

Fig. 3 (a) XRD pattern and (b) FT-IR spectrum of BHA400/3 catalyst.

708 cm^{-1}, 620 cm^{-1}, and 441 cm^{-1} are related to the stretching vibrations of M–O bonds (M: K, Ca, and Mg), which suggests the presence of metal oxides in the composition of the synthesized catalyst.[9,43] Therefore, the presence of CO_3^{2-} and M–O groups, attributed to the carbonates and metal oxides formed, is responsible for the catalytic activity observed in biodiesel synthesis, with these active sites previously identified in the XRD analysis. The formation of these phases is essential for the efficiency of the catalyst, as it provides the basic sites necessary for the efficient transesterification of triglycerides.

The surface morphology of the BHA400/3 catalyst was evaluated using SEM analysis, with selected images magnified at 1000×, 2500×, and 5000×, as shown in Fig. 4(a)–(c), respectively. The micrograph reveals a complex system of particle agglomerates distributed in irregular shapes and sizes, and it also shows spongy morphology after the thermal treatment applied to the RBBH. This morphology results in a significant increase in surface area, which favors greater interaction with the reagents.[21] Consequently, this improved structure contributes to obtaining biodiesel with a high ester content. The regions with intense brightness observed in the image may be caused by the presence of oxygenated materials from the metal oxides present in the BHA400/3 catalyst.[44] Similar morphological structures of catalysts derived from agro-industrial residues have been reported in the works developed by Nath *et al.*,[45] Changmai *et al.*,[16] and Eldiehy *et al.*,[40] which used banana peels (*Brassica nigra*), orange peels, and radish leaves (*Raphanus sativus* L.), respectively.

Fig. 5 illustrates the EDS spectrum and the mapping of the chemical elements present on the surface of the BHA400/3 catalyst. Fig. 5(a) shows the peaks of each identified element and their respective concentrations. Among all, the peak corresponding to potassium (K) stands out with a content of 13.51%, representing the major metal in the catalyst composition, followed by calcium (Ca) with 5.62%, magnesium (Mg) with 5.48%, and sodium (Na) with 0.30%, which contribute to the basic nature of the catalyst. Additionally, the other peaks correspond to silicon (Si), oxygen (O), and carbon (C) with contents of 0.31%, 38.8%, and 35.97%, respectively. These are related to silicates, oxides, and metal carbonates. Furthermore, the carbon (C) content may be associated with the carbonaceous species formed from the partial thermal decomposition of the RBBH used during the synthesis of the BHA400/3 catalyst. It is worth noting that high carbon contents are also reported in studies conducted by Pathak *et al.*,[46] Mares *et al.*,[9] and Changmai *et al.*,[16] showing carbon contents of 47.51%, 42.40%, and 32.5%, respectively.

In general, the chemical composition of the BHA400/3 catalyst differs when compared to other solid catalysts derived from various agro-industrial residues, such as those reported by Aleman-Ramirez *et al.*,[47] Basumatary *et al.*,[34] and Nath *et al.*[48] However, these variations depend on several factors, such as the nature of the raw material, climate, soil, geographical location, as well as the catalyst synthesis parameters. Additionally, it is important to highlight that the presence of potassium in high concentration contributes to the catalyst's good catalytic performance for biodiesel production.

The surface elemental mapping of the BHA400/3 catalyst shown in Fig. 5(b) and (c) reveals a homogeneous distribution of the chemical elements that compose it. In the analyzed area, potassium, symbolized in blue, has the highest density among the alkaline metals present in the material composition, followed by calcium in pink and magnesium in green. The region in red, representing carbon, is attributed to the metal carbonates formed and carbonaceous species resulting from the incomplete carbonization of RBBH after thermal treatment. Thus, the surface elemental analysis confirms that potassium is the most abundant metal in the BHA400/3 catalyst, present in the forms of oxides and carbonates, as previously evidenced by the XRD and FT-IR analyses.

Thermogravimetric analysis aims to investigate the behavior of the material when subjected to temperature variations, allowing the determination of intervals where mass changes occur. Fig. 6 shows the TG and DTG curves of the RBBH and the BHA400/3 catalyst. From the analysis of Fig. 6(a), which illustrates the TG/DTG curves of the RBBH, it is possible to observe three mass loss events, a similar thermal behavior as reported by Sarkar *et al.*[49] The first thermal decomposition event of the

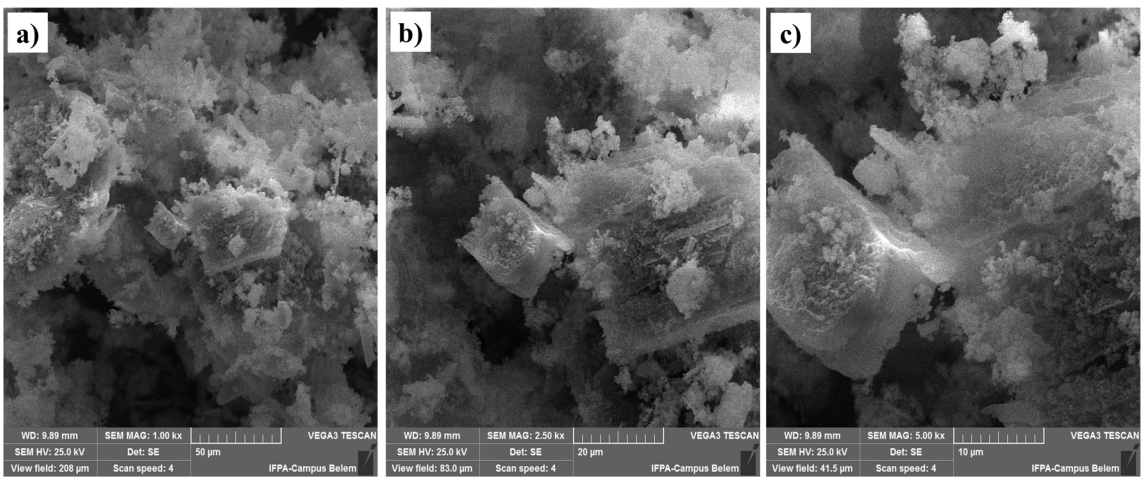

Fig. 4 SEM micrographs of BHA400/3 catalyst (a) 1000× magnification, (b) 2500× magnification and (c) 5000× magnification.

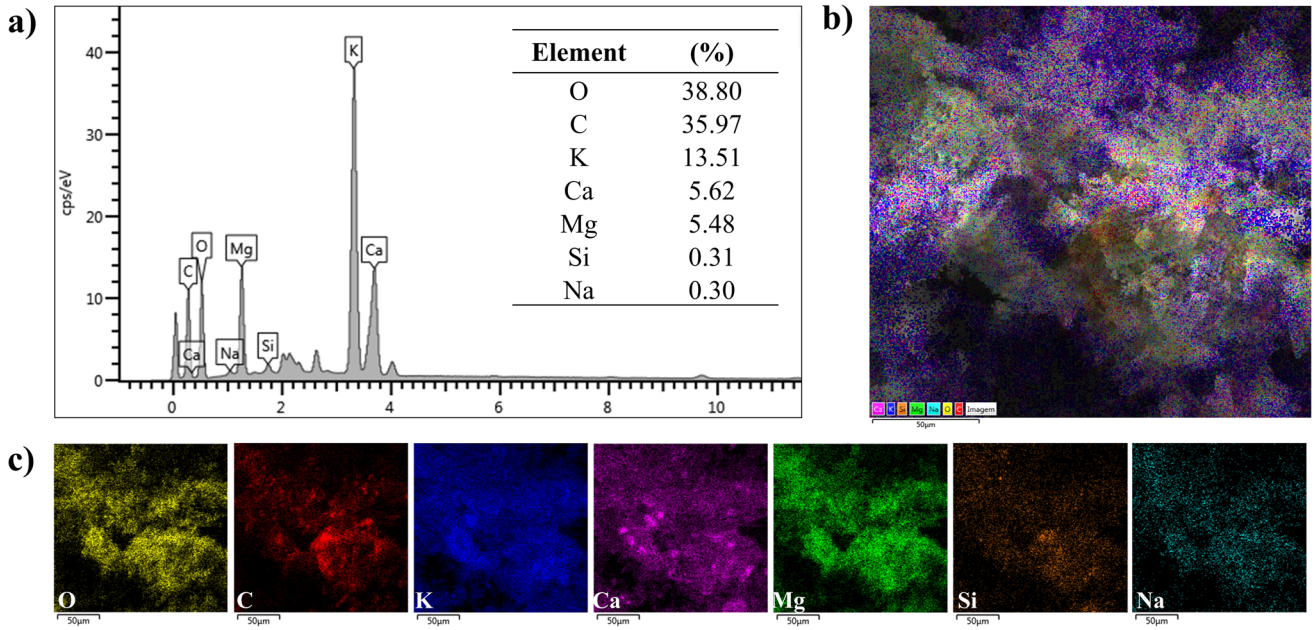

Fig. 5 (a) EDS spectrum, (b) and (c) surface elemental mapping of BHA400/3 catalyst.

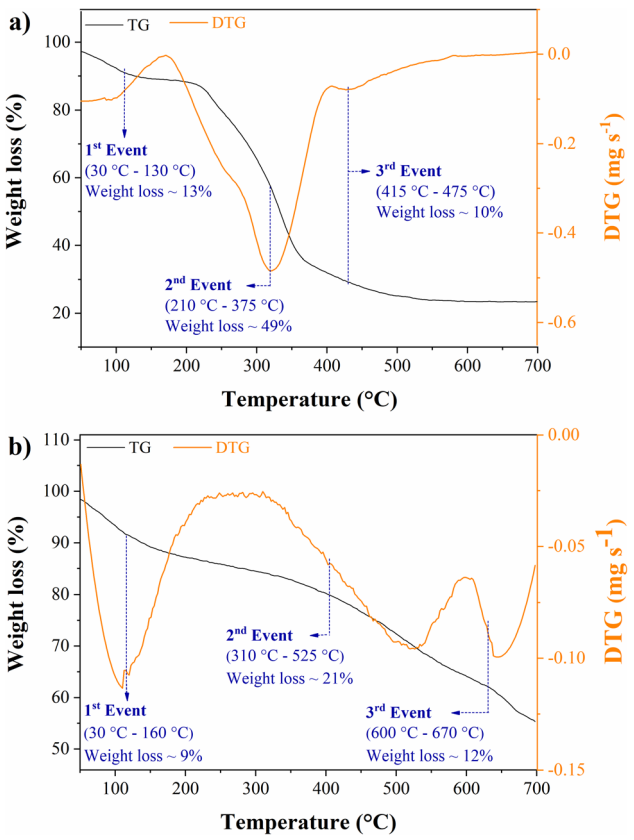

Fig. 6 TG/DTG curves of (a) RBBH and the (b) BHA400/3 catalyst.

RBBH occurs in the temperature range of 30–130 °C, with a mass loss of approximately 13%, and is related to the removal of moisture and low molecular weight compounds.[50] A second mass loss event was observed in the temperature range of 210–375 °C, corresponding to a value close to 49%. This significant mass loss event may be related to the degradation of carbonaceous materials, such as the decarboxylation of hemicellulose and cellulose, releasing CO and CO_2.[16,51] The third event occurs in the temperature range of 415–475 °C, representing a mass loss of around 10%, which can be attributed to the decomposition of metal carbonates and their gradual conversion into metal oxides.[52,53]

Fig. 6(b) shows the TG/DTG curves of the BHA400/3 catalyst, and three mass loss events are observed. The first event was observed in the temperature range of 30–160 °C, corresponding to a mass loss of about 9%, attributed to the desorption of physisorbed water in the material.[38] The second event represents a mass loss of 21% and occurs in the temperature range of 310–525 °C. This event may be attributed to the degradation of residual carbonaceous species that make up the BHA400/3 catalyst, releasing CO and CO_2.[50,54] In the third event, which occurs in the temperature range of 600–670 °C, a mass variation of about 12% is observed, related to the decomposition of carbonates resulting in the formation of metal oxides and the release of CO_2.[55,56]

3.3. Influence of reaction parameters on biodiesel synthesis

3.3.1. Influence of temperature. The variation of reaction parameters employed in biodiesel synthesis is shown in Fig. 7. The influence of the reaction temperature on the ester contents of biodiesel (Fig. 7(a)) was evaluated at temperatures of 60 °C, 75 °C, 90 °C, 105 °C, and 120 °C, with reaction time, molar ratio MeOH : oil, and catalyst concentration kept constant at 1.5 h, 20 : 1, and 6 wt%, respectively. Based on the results obtained, the temperatures of 60 °C and 75 °C resulted in ester content below 7%. However, when the reaction temperature is increased to 90 °C, the ester content rises significantly to 72.8% ± 0.26,

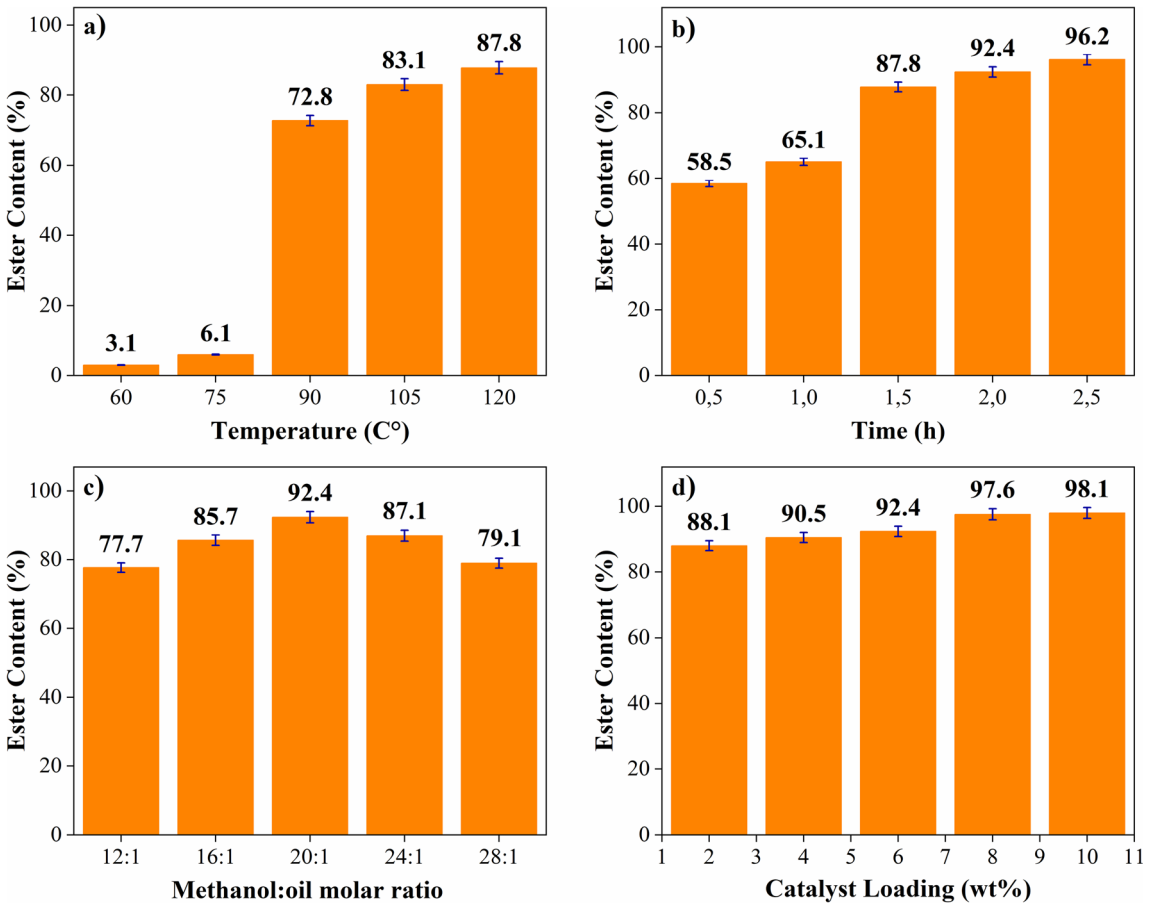

Fig. 7 Influence of (a) reaction temperature, (b) reaction time, (c) MeOH : oil molar ratio and (d) catalyst concentration on ester content.

representing an increase of approximately 65% compared to the ester contents of biodiesel produced at temperatures of 75 °C and 90 °C in the transesterification reaction. This significant increase in biodiesel ester content is explained by the rise in temperature in the reaction system, which reduces the viscosity of the reaction medium and, consequently, provides better homogeneity of the reagents and mass transfer within the system.[57,58]

Typically, an increase in reaction temperature leads to an increase in the ester content of the produced biodiesel, and this is evident from the ester contents of 83.1% ± 0.29 and 87.8% ± 0.32 obtained when the reactions were conducted at temperatures of 105 °C and 120 °C, respectively. These results represent an average increase in ester content of about 20% when compared to the biodiesel obtained at 90 °C. Additionally, it is worth noting that the reactions were conducted in a closed system, and thus, increasing the temperature causes the methanol to vaporize, leading to an increase in internal pressure. This can cause the fluids to move at a higher velocity, increasing the kinetic energy of the reactant molecules, which then interact more strongly with each other. These interactions increase the probability of effective collisions between reactant molecules, which can break bonds and form new products, thereby efficiently promoting biodiesel production.[57,59] Therefore, the reaction temperature of 120 °C was selected for the continuation of this study.

3.3.2. Influence of reaction time. The influence of reaction time on biodiesel production was evaluated over a range of 0.5 to 2.5 hours, using a temperature of 120 °C, a molar ratio of MeOH : oil of 20 : 1, and 6 wt% catalyst, as shown in Fig. 7(b). The results indicate that the longer reaction time (2.5 hours) promoted a high ester content in the biodiesel, reaching 96.2% ± 0.29. Generally, increasing the reaction time leads to an increase in ester content, due to the extended contact time between the reagents (oil and methanol) and the catalyst. However, biodiesel produced with a reaction time of 2 h achieved an ester content of 92.4% ± 0.24, indicating a slight variation of less than 4% compared to the value obtained at 2.5 h. This trend and behavior are similar to those discussed in the studies by Yuliana *et al.*[60] and Lin *et al.*[61] which highlight the importance of reaction time in effectively promoting molecular interaction between the reagents and their respective catalysts, in order to initiate the reaction and convert as much soybean oil as possible into biodiesel. Thus, considering the minimal difference in ester content values and the desire to minimize operational costs in the process, a reaction time of 2 h was selected for the continuation of the study.

3.3.3. Influence of molar ratio MeOH : oil. The transesterification reaction is reversible, and to shift the equilibrium

towards the formation of methyl esters and glycerol, an excess of alcohol is required. Therefore, the molar ratio MeOH : oil becomes a significant factor influencing ester content. The effect of different molar ratios of MeOH : oil, ranging from 12 : 1 to 28 : 1, was evaluated while keeping the other variables constant: reaction temperature at 120 °C, reaction time of 2 h, and 6 wt% of catalyst.

Fig. 7(c) shows that increasing the molar ratio MeOH : oil from 12 : 1 to 20 : 1 leads to biodiesel with ester contents of 77.7% ± 0.22 and 92.4% ± 0.28, representing an approximately 15% increase in ester content. However, it is noted from Fig. 7(c) that reactions processed using molar ratios of 24 : 1 and 28 : 1 resulted in biodiesel with ester contents of 87.1% ± 0.26 and 79.1% ± 0.21, respectively, indicating a decrease in ester content compared to the biodiesel obtained using a molar ratio of 20 : 1. This is due to the fact that higher molar ratios lead to an excess of methanol in the system, resulting in dilution of the reaction medium, which limits the interaction of the reagents with the active sites of the catalyst, consequently leading to a decrease in the ester content of the biodiesel.[62]

These experimental data showed similarities to those obtained by Khan *et al.*,[63] who reported that biodiesel with low ester contents could be caused by disproportionate amounts of alcohol in the reaction medium, which can dilute glycerol, causing reverse reactions. Thus, the molar ratio MeOH : oil of 20 : 1 was selected and used in all subsequent reactions as part of the optimal condition for achieving maximization of ester content in biodiesel.

3.3.4. Influence of catalyst concentration. The amount of catalyst used in the reaction medium impacts the rate at which the reactants are consumed and the ester content. To achieve maximum to ester content, different concentrations of the BHA400/3 catalyst (2, 4, 6, 8, and 10 wt%) were evaluated in the transesterification reaction, under fixed conditions of 120 °C temperature, 2 h reaction time, and a MeOH : oil molar ratio of 20 : 1. From the analysis of Fig. 7(d), it is possible to observe an increasing trend in the ester contents of the biodiesel produced as the catalyst concentration in the reaction increases, with particular emphasis on catalyst concentrations of 4% or higher, which resulted in ester contents exceeding 90%. This may be related to the greater number of active sites available in the reaction medium, maximizing the contact between the reactants and the catalyst surface.[64]

Fig. 7(d) also shows that using 8% and 10% of the BHA400/3 catalyst resulted in biodiesel with ester contents of 97.6% ± 0.33 and 98.1% ± 0.35, respectively, values that are extremely close. This indicates that the maximum yield is achieved with a catalyst concentration around 8%, and using higher concentrations of catalyst in the transesterification reaction will not significantly increase the ester content.[50] Therefore, the 8% catalyst concentration, which proved efficient in biodiesel production, was selected for further study.

3.4. Study of BHA400/3 catalyst reusability

Heterogeneous catalysts offer distinct advantages over homogeneous catalysts, one of which is the potential for reuse in transesterification reactions—a crucial factor that makes them favorable for industrial applications due to cost reductions in biodiesel production.[65] The reusability study of the BHA400/3 catalyst was conducted under optimal reaction conditions: a temperature of 120 °C, a reaction time of 2 h, a MeOH : oil molar ratio of 20 : 1, and a catalyst concentration of 8 wt%. The results are shown in Fig. 8.

Based on the data presented in Fig. 8, it is evident that the BHA400/3 catalyst exhibited a reduction in catalytic activity over successive reaction cycles. The second reaction cycle resulted in biodiesel with a 57.1% ± 0.38 ester content, a reduction of approximately 38% compared to the biodiesel produced in the first cycle, which had a 95.6% ± 0.51 ester content. In the third cycle, the biodiesel achieved an even lower ester content of 27.4%. This decrease in ester content indicates partial deactivation of the catalyst, which may be attributed to the leaching of surface active sites into the reaction medium.[16] This leaching effect restricts the reactants' access to the basic active sites, particularly the vegetable oil, which consists of long hydrocarbon chains, causing difficulties in efficiently processing the reaction to produce biodiesel. It is worth noting that despite the decrease in ester content in the biodiesel over the reaction cycles, the value remained significantly higher than of biodiesel produced without the catalyst (4.2% ± 0.03 ester content in the control reaction). Although the BHA400/3 catalyst shows a reduction in ester content, it still exhibits partial catalytic activity, as the biodiesel produced had an ester content above 50%. Therefore, it is feasible to consider the regeneration of the BHA400/3 catalyst to recover its catalytic activity by increasing the number of active sites on the catalyst surface.

3.5. Study of BHA400/3 catalyst regeneration

3.5.1. Influence of calcination temperature. The BHA400/3 catalyst, which showed partial deactivation after the second reaction cycle, was recovered and subjected to a doping process with KOH through wet impregnation to enhance its catalytic

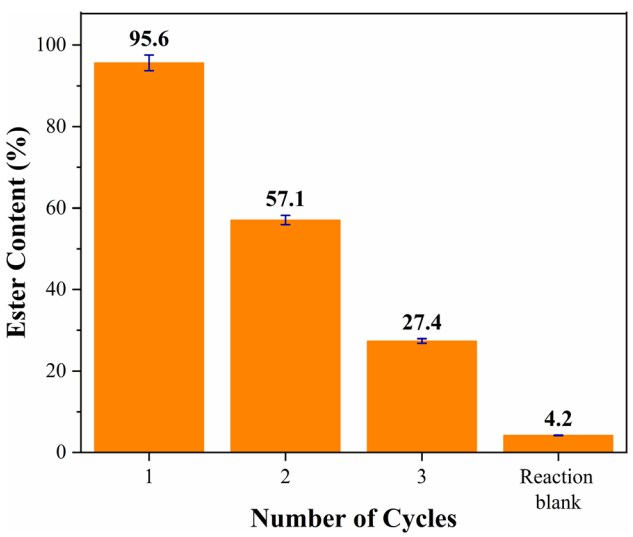

Fig. 8 Reusability study of BHA400/3 catalyst.

activities. The catalyst regeneration study considered data reported by Foroutan *et al.*,[24] who synthesized an efficient heterogeneous catalyst for biodiesel production from *Luffa cylindrica* biomass ash impregnated with KOH, and by Hernández *et al.*,[66] who reported a heterogeneous catalyst synthesized from the carbonization of coconut shells, impregnated with KOH and $Ca(NO_3)_2$, capable of achieving biodiesel with ester content above 90%.

Therefore, to improve catalytic activity and reduce operational costs of biodiesel production, the catalyst regeneration process was optimized with respect to temperature and potassium concentration. In this phase, the best calcination temperature (200, 300, and 400 °C) for the regeneration of the BHA400/3 catalyst using KOH as the doping agent was evaluated, with the calcination time fixed at 3 h. It is worth noting that the reactions were conducted under the optimal conditions defined previously, and the ester contents of the biodiesels produced in this study phase are presented in Fig. 9.

In general, Fig. 9 shows that the regenerated catalysts calcined at 200, 300, and 400 °C exhibited enhanced catalytic activities. Initially, considering only the first reaction cycles with the BHA400/3-R catalysts, the calcination temperatures of 200 and 300 °C stand out, demonstrating greater effectiveness of these catalysts after the regeneration process, promoting biodiesels with ester contents of 99.9% ± 0.33 and 97.2% ± 0.45 (cycle 1 BHA400/3-R), respectively. This represents an increase of about 40% in esters when compared to the ester content of biodiesel obtained in cycle 2 with the BHA400/3 catalyst, which was 57.1% ± 0.11 (cycle 2 BHA400/3). However, when the BHA400/3-R catalyst treated thermally at 400 °C was reused in the reaction cycle study, biodiesel with an ester content of 81.8% ± 0.31 was obtained, representing about 15% less ester content compared to the other catalysts treated at 200 and 300 °C.

This downward trend becomes more pronounced when analyzing the results from the subsequent reaction cycles. The catalysts treated at 200 and 300 °C used in cycle 2 BHA400/3-R resulted in biodiesels with ester contents of 96.2% ± 0.28 and 92.7% ± 0.3, respectively, while the catalyst treated at 400 °C yielded a biodiesel with an ester content of 67.1% ± 0.21, representing a catalytic performance loss of about 25%. Thus, the lower performance of the catalyst treated at 400 °C may be related to the fact that this temperature leads to partial degradation of the carbonaceous species present in the BHA400/3 catalyst, causing a reduction in surface area and resulting a smaller distribution of the active phases formed on the catalyst surface during the calcination step. Therefore, it is evident that increasing the calcination temperature did not lead to significant improvements in catalytic activity.[2]

On the other hand, the catalysts calcined at 200 and 300 °C exhibited good catalytic stability, with high ester content to biodiesel. After the thermal treatment, it was observed that the carbonaceous species remained stable, indicating that at temperatures up to 300 °C, the carbonaceous compounds remained intact. Therefore, the increased catalytic activity of the catalysts treated at 200 and 300 °C can be explained by the formation of potassium carbonate and oxide phases due to the thermal treatments performed, resulting in an increase in the number of active sites available for the reaction, along with the preservation of the carbonaceous compounds present in the BHA400/3 catalyst. However, it is noteworthy that the catalyst regenerated at 300 °C showed greater catalytic stability, resulting in biodiesel with an ester content of 76.1% ± 0.17 when applied in cycle 3 BHA400/3-R, while the catalyst calcined at 200 °C produced biodiesel with 65.8% ± 0.19 ester content in the same reaction cycle after regeneration, a catalytic activity loss of over 10%. Therefore, the calcination temperature of 300 °C is considered the most suitable for the regeneration process of the BHA400/3-R catalyst.

3.5.2. Influence of potassium concentration. KOH was selected as the doping agent for the regeneration process of the BHA400/3 catalyst because potassium (K) is the predominant

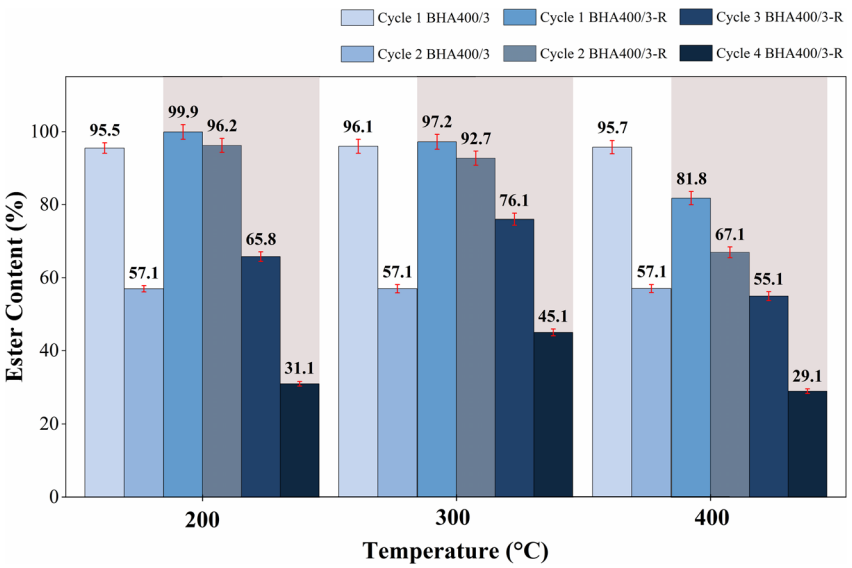

Fig. 9 Influence of calcination temperature on the regeneration of BHA400/3 catalyst in biodiesel production.

metallic element in the material's composition, as previously demonstrated. Differently from conventional homogeneous catalysis, in which large quantities of KOH are used, generating significant waste, this study employs only a minimal amount to efficiently restore catalytic activity. Furthermore, this approach not only provides high performance, but also makes the regeneration process more sustainable and economical.

Therefore, when the BHA400/3 catalyst showed partial deactivation in cycle 2 (with an ester content of 57.1% ± 0.11), the catalyst was recovered and subjected to the regeneration process by wet impregnation of an aqueous KOH solution, where the evaluated potassium concentrations were 5, 10, and 15 wt%. The ester contents of the biodiesels obtained in this study are shown in Fig. 10.

In general, Fig. 10 shows that the regeneration process with any studied (K) concentration positively affects the catalyst's performance, as the concentrations used in the study increase the number of accessible alkaline sites for the transesterification of triglycerides, leading to an increase in the ester content of the biodiesels. However, some differences can be noted due to the use of different (K) concentrations in the regeneration process. For example, only concentrations above 10 and 15 wt% of K led to biodiesels with ester contents above 97.0% in cycle 3, specifically 97.2% ± 0.45 and 99.9% ± 0.33, respectively. In contrast, the 5 wt% K concentration used in the regeneration process promoted an ester content of 93.2% ± 0.32. This difference in catalytic activity becomes more evident when comparing the ester contents of the biodiesels produced in cycle 4, as the catalyst treated with 5 wt% resulted in an ester content of 85.7% ± 0.24, while the catalysts regenerated with 10 and 15 wt% maintained catalytic activity with biodiesels having ester contents above 92%. It is important to note that this trend of catalytic activity loss between reaction cycles is strongly marked when analyzing the ester contents of the biodiesels produced in cycle 5, where the catalysts treated with (K) concentrations of 5, 10, and 15 wt% led to ester content of 69.8 ± 0.15, 76.1, ± 0.18 and 79.6% ± 0.23, respectively.

The percentage difference in ester content can be attributed to factors such as non-homogeneous distribution of active phases on the catalyst surface or related to weak anchoring interactions of metallic groups on the carbonaceous species, which favors the leaching of active basic groups into the reaction medium and, consequently, causes a reduction in catalytic activity, as reported in the study described by Hernández *et al.*[67] Thus, it is observed that the 10 and 15 wt% K concentrations in the regeneration process of the BHA400/3 catalyst resulted in better catalytic activity and stability. However, among these concentrations used, the percentage difference in the ester content of the biodiesels is minimal (less than 4% in cycle 5 and approximately 1% in cycle 6). Therefore, to select the best regeneration parameter for the catalyst, along with the fact of minimizing operational costs, the 10 wt% potassium concentration was selected as the most efficient concentration for restoring the catalytic activity of the BHA400/3 catalyst. Therefore, the optimal regeneration condition for the catalyst was calcination at 300 °C, with a potassium concentration of 10 wt%, under 3 h of thermal treatment.

These results highlight the advantage of using a heterogeneous catalyst with a well-defined regeneration process, in contrast to homogeneous catalysis, which requires large quantities of KOH and leads to excessive consumption of reagents and the generation of effluents. Thus, by using only 10% by weight of KOH in the regeneration process, the study demonstrates that it is possible to obtain a catalyst with stable and high catalytic performance over several cycles, significantly reducing chemical waste. This reinforces the potential of biomass-derived catalysts as a sustainable alternative for the industrial production of biodiesel.

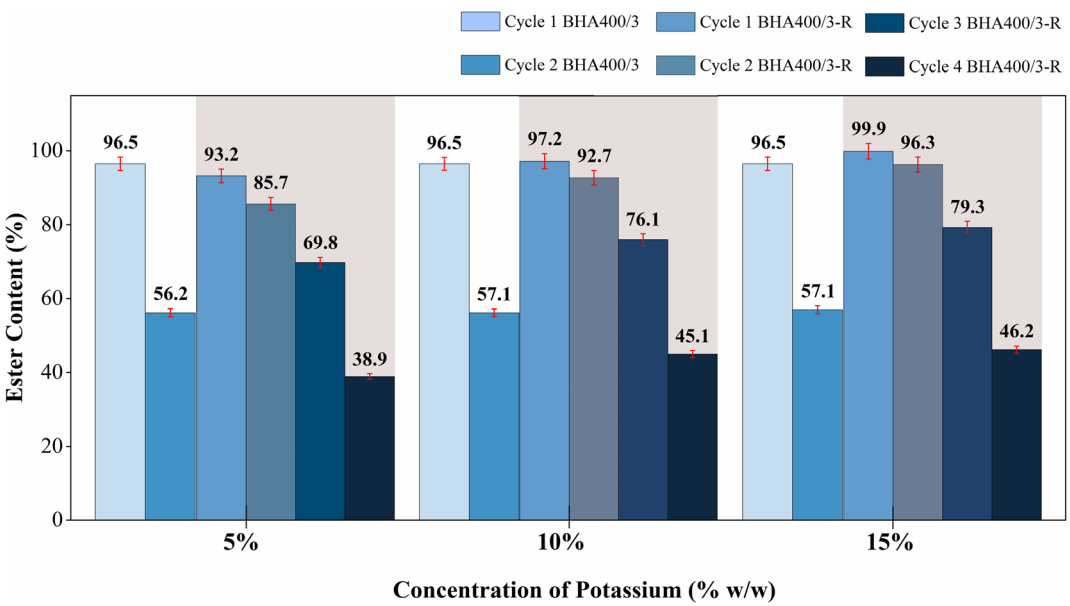

Fig. 10 Influence of potassium concentration variation in the regeneration study of BHA400/3 catalyst.

3.6. Characterization of catalyst BHA400/3-R

After cycle 2 of the reaction, the BHA400/3 catalyst was partially deactivated in biodiesel production, showing an ester content of 57.1% ± 0.11, as previously mentioned. However, it is important to highlight that the basicity was 2.85 mmol g^{-1} ± 0.024, a decrease of 1.99 mmol g^{-1} ± 0.018 compared to the basicity of the catalyst in cycle 1. This suggests that as the BHA400/3 catalyst is subjected to a new transesterification cycle, the available active surface sites for the reaction are leached into the reaction medium and/or during its purification. Therefore, a regeneration process was performed on the catalyst, now referred to as BHA400/3-R. After this step, the basicity of BHA400/3-R was determined to be 4.86 mmol g^{-1} ± 0.031, indicating a significant increase in the active sites in the catalyst composition. Thus, BHA400/3-R was employed in the transesterification reaction, producing biodiesels with ester contents of 97.2% ± 0.45, 92.7% ± 0.3, 76.1% ± 0.17, and 45.1% ± 0.1, respectively. These results with high ester content are correlated with the increase in the catalyst's basicity due to the impregnation of active sites and thus confirm the efficiency of the applied method when the catalyst showed partial deactivation. This allows for its reuse in biodiesel production.

The X-ray diffraction (XRD) spectrum of BHA400/3-R is shown in Fig. 11(a). The crystalline compounds present in the BHA400/3-R catalyst are identified from the XRD analysis by comparing the 2θ values obtained with data reported in the literature. According to the analysis data, the impregnation of potassium hydroxide in the partially deactivated catalyst was successful. The identified groups included carbonates, oxides, and hydroxides of alkaline metals. Peaks at $2\theta = 28.18°$, 29.53°, 34.33°, and 41.96° are attributed to the K_2CO_3 phase, with particular emphasis on the peak observed at $2\theta = 29.53°$ due to its high intensity. The presence of this phase is particularly relevant, as alkaline carbonates are known for their ability to provide active basic sites, promoting biodiesels with a high ester content. The results related to the K_2CO_3 phase are similar to values reported in studies by Das *et al.*[66] and Prajapati *et al.*[50] However, other phases were also identified, such as K_2O, CaO, MgO, $CaCO_3$, and $Ca(OH)_2$, as previously demonstrated in the XRD pattern collected for the BHA400/3 catalyst.

The FT-IR spectrum of the BHA400/3-R catalyst is shown in Fig. 11(b). The broad band located in the spectrum at 3291 cm^{-1} corresponds to the stretching vibrations of the O–H bond due to water molecules adsorbed on the catalyst surface,[48,68] while the intense band at 1436 cm^{-1} is attributed to the stretching and bending vibrations of the C–O bond, suggesting the presence of carbonate ions. This functional group, in particular, plays a crucial role in catalytic performance, since carbonate species (C–O bonds) are directly associated with the formation of basic active sites, which are essential for promoting transesterification reactions.

This characteristic band was also observed for heterogeneous catalysts derived from residual biomass in different studies, such as those by Zhao *et al.*,[69] Changmai *et al.*,[16] and Basumatary *et al.*[70] Another band representing the carbonate group is located at 873 cm^{-1}, attributed to C–O bending vibrations.[45]

The band at 1058 cm^{-1} can be attributed to the symmetric stretching of C–O due to the breakdown and depolymerization of lignocellulosic materials (lignin and cellulose) present in the biomass.[41] Meanwhile, the bands located at 716 cm^{-1}, 554 cm^{-1}, and 467 cm^{-1} in the spectrum are attributed to the stretching vibrations of the M–O bond groups (M: K, Ca, and Mg), with the 716 cm^{-1} band corresponding to K–O.

Elemental identification was performed using complementary EDS analysis, as shown in Fig. 12. Fig. 12(a) presents the collected data for the analyzed region, including the peaks of each chemical element and their respective percentages. It is observed that the most predominant peak corresponds to potassium (K) with a content of 20.11%, making it the major metal in the catalyst composition, as it is the metal of interest due to its addition on the material's surface. Other metals are identified with lower percentages: Mg at 5.72%, Ca at 7.37%, Si at 0.45%, and Na at 0.31%. Additionally, another relevant observation shown in Fig. 12(b) and (c) is the distribution and

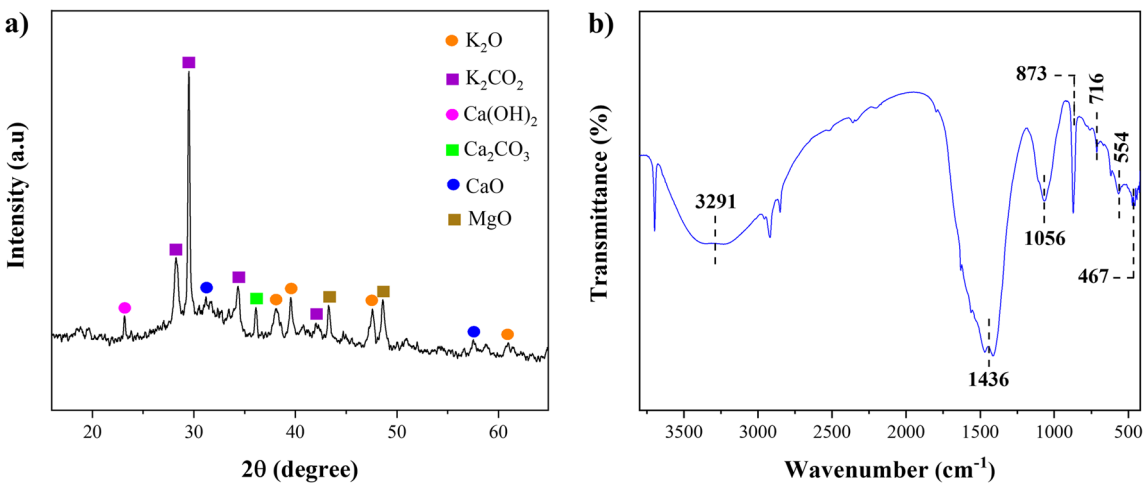

Fig. 11 (a) XRD pattern and (b) FT-IR spectrum of BHA400/3-R catalyst.

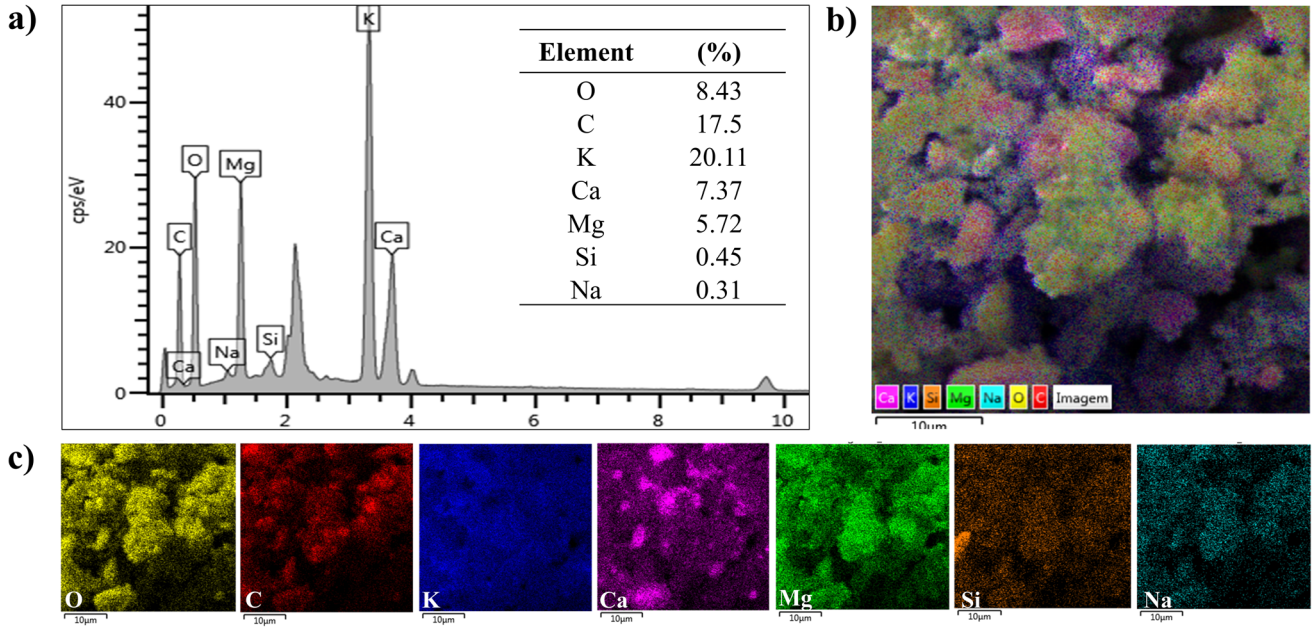

Fig. 12 (a) EDS spectrum, (b) and (c) surface elemental mapping of BHA400/3-R catalyst.

density of the metals, where K presents homogeneity in surface distribution and higher density. Therefore, the elemental analysis indicates the efficiency of the impregnation method due to the higher amount of K in the BHA400/3-R catalyst, mainly in the form of carbonate, as previously shown by the XRD and FT-IR analyses.

3.7. Physicochemical properties of biodiesel

The biodiesel obtained from soybean oil under optimal reaction conditions, using the basic catalyst BHA400/3, was characterized by its physicochemical properties. The results were compared with the values defined by the international standard ASTM D6751, as shown in the Table 1.

The biodiesel recorded density and kinematic viscosity values of 0.880 g cm^{-3} and 4.3 mm^2 s^{-1}, respectively. Based on these results, the obtained biodiesel exhibited values within the limits established by ASTM D6751. Additionally, these values indicate that the biodiesel will not cause issues in the mechanical system of a vehicle, as these properties are directly related to the fuel's quality and fluidity, atomization during injection into the combustion chamber, and the molecular structure of the biodiesel.[65] The acid value and copper corrosion properties of the biodiesel were recorded at 0.17 mg KOH per g and 1a, respectively, which are relatively lower than the maximum limits set by the standard. This means that the synthesized biodiesel will not cause corrosive action that could damage the metal parts of the engine.[9,65]

The flash point is a crucial property of biodiesel as it determines its volatility. This parameter allows for the classification of the material's flammability, being essential to ensure safety during storage and transport. An adequate flash point ensures that the fuel does not present high fire risks under normal handling conditions. The flash point for the studied biodiesel was 152 °C, a value similar to those reported by Arumugam and Sankaranarayanan,[54] Das *et al.*,[66] and Changmai *et al.*[16] for biodiesels obtained from soybean oil. The cold filter plugging point (CFPP) of the biodiesel is a parameter that determines the minimum temperature at which the fuel undergoes partial solidification during cooling. This characteristic is related to both the degree of saturation and the hydrocarbon chain length

Table 1 Physicochemical properties of soybean biodiesel synthesized using the BHA400/3 catalyst and the limits specified by ASTM D6751 standard[a]

Biodiesel properties	Unit	Test methods	ASTM D6751 limits	Present study
Kinematic viscosity (at 40 °C)	mm^2 s^{-1}	ASTM D445	1.9–6.0	4.3
Density (at 20 °C)	g cm^{-3}	ASTM D6890	0.875–0.900	0.880
Acid value	mg KOH per g	ASTM D664	0.5 max	0.17
Copper strip corrosion	—	ASTM D130	3 max	1
Flash point	°C	ASTM D93	130 min	152
Cold filter plugging point	°C	ASTM D6371	NS	0

[a] NS: not specified.

of the esters. As indicated in Table 1, the observed value for the cold filter plugging point was 0 °C, suggesting that the biodiesel synthesized in this study can be transported and used in colder regions.

Therefore, the physicochemical characterization of the biodiesel showed results in compliance with ASTM D6751 standards, demonstrating the excellent quality of the soybean biodiesel synthesized from the BHA400/3 catalyst under optimal conditions.

3.8. Investigation of the performance of the BHA400/3 catalyst in the transesterification of different oils

Table 2 shows the ester content of biodiesels synthesized from different oilseed feedstocks, ranging from high to low quality, evidencing the influence of the acid value as a parameter for basic heterogeneous catalysis. It also emphasizes the feasibility of using bean husks as an alternative raw material for biodiesel production, using different vegetable oils.

Based on the data presented in Table 2, it can be seen that the reactions using soybean, corn, sunflower and palm oil, which are considered neutral, resulted in biodiesels with relatively high ester content (above 90%). This result is due to the fact that these oils have a low acid value, which favors more efficient biodiesel production. Vegetable oils with a low concentration of free fatty acids (FFA) minimize the occurrence of undesirable reactions, allowing transesterification to take place without significant interference.[71] Studies on the production of biodiesel from sunflower, corn and palm have reported ester contents of 80%, 94% and 98.5%, respectively.[72–74] Thus, the application of the basic heterogeneous catalyst to these raw materials is expected to result in high product purity.

In contrast, the ester content of biodiesel synthesized from used cooking oil was only 3.1% (±0.15). This result is due to the fact that used cooking oil has a significantly higher acid value, due to the thermal degradation and oxidation of triglycerides throughout its use. The increase in acidity raises the concentration of free fatty acids (FFA), which react with the basic catalyst, favoring undesirable secondary reactions such as saponification.[75] The formation of soaps reduces the availability of the catalyst for transesterification, which makes phase separation difficult and compromises the purity of the synthesized biodiesel.[76] As a result, the ester content obtained tends to be significantly lower than that of neutral vegetable oils.

Table 2 Ester content obtained in the transesterification of different oils using the BHA400/3 catalyst

Feedstock	Acid value (mg KOH per g)	Ester content (%)
Soybean oil	0.18 ± 0.01	97.6 ± 0.35
Corn oil	0.25 ± 0.01	91.5 ± 0.55
Sunflower oil	0.21 ± 0.02	95.7 ± 0.45
Palm oil	0.22 ± 0.01	96.3 ± 0.35
Used cooking oil	4.5 ± 0.02	3.1 ± 0.15

Therefore, the choice of feedstock has a fundamental role to make in the performance of the basic heterogeneous catalyst, since the presence of free fatty acids in high concentrations in vegetable oil not only reduces the efficiency of the catalyst, but also requires additional steps in the processing of biodiesel to minimize losses and improve the quality of the final product. Furthermore, the use of bean husks could be a low-cost and sustainable alternative, broadening the options of renewable sources for biodiesel production.

3.9. Comparison of the catalytic activity of different biomass-derived basic catalysts applied in biodiesel production

Table 3 presents a comparison of the performance of the BHA400/3 and BHA400/3-R catalysts with various heterogeneous catalysts from biomass sources found in the literature. Table 3 outlines the synthesis parameters of the catalysts, as well as the optimal reaction parameters for biodiesel production and ester content. Additionally, it covers the regeneration results for some catalysts, including the number of reaction cycles and ester content of the biodiesel.

Firstly, based on the data regarding the synthesis parameters of different catalysts, it is evident that the thermal treatment applied in RBBH (400 °C/3 h) involves milder carbonization conditions compared to the other synthesized catalysts. This results in reduced costs during biodiesel production, as less energy is required for biomass carbonization. Moreover, the BHA400/3 catalyst demonstrates good catalytic activity, achieving an ester content of 97.2% ± 0.45, which is comparable to other biodiesels produced by the catalysts reported in Table 3, albeit under higher carbonization conditions, as seen in the synthesis from açaí seeds,[9] leguminous plant shells,[49] and banana peels,[65] which are treated at 800 °C for 4 h, 700 °C, and 600 °C for 4 h, respectively.

Another point to note is regarding the optimal reaction parameters for biodiesel synthesis, which show similarities between the studies presented in Table 3 and the results of this work. According to the results reported by the authors, satisfactory ester content were achieved when using ashes as a heterogeneous catalyst without requiring additional chemical steps during the material synthesis process, such as tucumã peel with an ester content of 97.3%,[77] banana peels with an ester content of 92.3%,[65] and *Moringa* leaves with an ester content of 86.7%.[47]

This study addresses the regeneration process *via* wet impregnation. Based on Table 3, it is noted that there is a lack of literature addressing this aspect of heterogeneous catalysis, with only studies on murici seed and açaí seed biomass.[9,78] Therefore, when comparing these studies with the present work, the results show a certain similarity due to the high ester content achieved, as well as good catalytic stability throughout the reaction cycles. This is evidenced by the ester content results of 97.2% ± 0.45 and 4 reaction cycles (present study), 96.71% and 5 reaction cycles (murici seed), and 94.0% and 5 reaction cycles (açaí seed). Thus, this highlights the viability of the wet impregnation method to recover catalytic activity, as active

Table 3 Application of heterogeneous catalysts derived from biomass in biodiesel production[a]

	Catalyst synthesis	Reaction conditions				
Biomass precursor	T (°C); t (h)	T (°C); t (h); RM; CC (wt%)	Ester content (%)	Cycles after regeneration	Ester content (%)	Ref.
Parkia speciosa shells	700; NS	40; 3; 15 : 1; 5	96.4	—	—	50
Tucumã shells	800; 4	80; 4; 15 : 1; 1	97.3	—	—	72
Musa acuminata banana peels	600; 4	70; 4; 15 : 1; 1	92.3	—	—	67
Moringa leaves	500; 2	65; 2; 6 : 1; 6	86.7	—	—	48
Ostrich bones	900; 4	60; 4; 15 : 1; 5	90.56	—	—	74
Birch bark	NS	60; 3; 12 : 1; 3	88.06	—	—	75
Lemna perpusilla Torrey	500; NS	65; 5; 9 : 1; 5	89.4	—	—	76
Murici seeds	NS	75; 1.5; 20 : 1; 5	97.2	5	96.71	73
Açaí seeds	800; 4	100; 1; 18 : 1; 12	98.6	5	94.0	9
Bean husk	400; 3	120; 2; 20 : 1; 8	97.6	4	97.2	This study

[a] T: reactional temperature; t: reactional time; RM: molar ratio; CC: catalyst concentration; NS: not specified.

components were added to the solid material's surface. Therefore, the results of this study display a consistent trend reported in the literature, further demonstrating the effectiveness of the catalyst applied in biodiesel production and validating the use of RBBH in synthesizing a basic heterogeneous catalyst.

4. Conclusion

This study evaluated the performance of the BHA400/3 catalyst, synthesized at 400 °C for 3 h, which led to a biodiesel with a maximum ester content of 97.6% ± 0.45 under optimized conditions (120 °C, 2 h, 20 : 1 and 8% catalyst). Characterization of the material revealed that it is mainly composed of alkali metals combined with oxygen and carbonates, such as K_2O, K_2CO_3, CaO, MgO and $CaCO_3$, with K_2O and K_2CO_3 acting as the main basic sites responsible for the high ester content. However, after two reaction cycles, the catalyst showed a reduction in ester content, but was effectively regenerated with KOH and maintained good performance in three successive cycles. In addition to its catalytic efficiency, bean husks stood out as a precursor which, when subjected to heat treatment, proved to be a sustainable and economical alternative for biodiesel production. In addition, the regenerability and stability of the catalyst in multiple cycles highlight its applicability in industrial processes, contributing to cost reduction and waste minimization. In this way, the process is not only scalable, but also represents an environmentally and economically attractive solution for large-scale biodiesel production.

Data availability

The datasets generated and analyzed in this current study are available from the corresponding author upon reasonable request.

Author contributions

Izadora de Araújo Sobrinho: conceptualization, methodology, investigation, visualization, formal analysis, writing – original draft. Thaíssa Saraiva Ribeiro: methodology, resources, investigation. Ane Caroline Dias e Silva: methodology, resources, investigation. Matheus Arrais Gonçalves: methodology, esources, investigation. Geraldo Narciso da Rocha Filho: supervision. Leyvison Rafael Vieira da Conceição: conceptualization, visualization, supervision, project administration, writing – review & editing.

Conflicts of interest

There are no conflicts of interest to declare.

Acknowledgements

The authors acknowledge the use of the facilities at Laboratory of Catalysis and Oil Chemistry (LCO/UFPA), Research Laboratory and Fuel Analysis (LAPAC/UFPA), X-ray Diffraction Laboratory (PPGF/UFPA), Laboratory of Vibrational Spectroscopy and High Pressures (LEVAP/UFPA) and Laboratory of Metallurgy of IFPA. The authors also thank the Graduate Program in Chemistry of the Federal University of Pará (PPGQ/UFPA), Coordination for the Improvement of Higher Education Personnel (CAPES) and Pro-Rectory for Research and Post-Graduated (PROPESP/UFPA).

References

1 L. Wang, H. Wang, J. Fan and Z. Han, Synthesis catalysts and enhancement technologies of biodiesel from oil feedstock – a review, *Sci. Total Environ.*, 2023, **23**, 166982, DOI: 10.1016/j.scitotenv.2023.166982.

2 P. Saetiao, N. Kongrit, C. K. Cheng, J. Jitjamnong, C. Direksilp and N. Khantikulanon, Catalytic conversion of palm oil into sustainable biodiesel using rice straw ash supported-calcium oxide as a heterogeneous catalyst: process simulation and techno-economic analysis, *Case Stud. Chem. Environ. Eng.*, 2023, **8**, 100432, DOI: 10.1016/j.cscee.2023.100432.

3 V. Khiangte, S. Lalhmangaihzuala, Z. T. Laldinpuii, L. Nunnemi, R. B. Muthukumaran and K. Vanlaldinpuia, Novel dragon fruit peel ash-derived solid catalyst for biodiesel production and PET waste recycling, *Bioresour. Technol. Rep.*, 2023, **24**, 101663, DOI: 10.1016/j.biteb.2023.101663.

4 A. Tizvir, G. R. Molaeimanesh, A. R. Zahedi and S. Labbafi, Optimization of biodiesel production from microalgae and investigation of exhaust emissions and engine performance for biodiesel blended, *Process Saf. Environ. Prot.*, 2023, **175**, 319–340, DOI: 10.1016/j.psep.2023.05.056.

5 B. Maleki, B. Singh, H. Eamaeili, Y. K. Venkatesh, S. S. A. Talesh and S. Seetharaman, Transesterification of waste cooking oil to biodiesel by walnut shell/sawdust as a novel, low-cost and green heterogeneous catalyst: optimization via RSM and ANN, *Ind. Crops Prod.*, 2023, **193**, 116261, DOI: 10.1016/j.indcrop.2023.116261.

6 K. Saikia, N. S. Moyon, R. Piloto-Rodríguez, F. Chai, S. Basumatary and S. L. Rokhum, Process optimization and kinetic studies of Musa glauca catalyzed biodiesel production, *Sustainable Chem. Pharm.*, 2023, **36**, 101271, DOI: 10.1016/j.scp.2023.101271.

7 V. S. Nagtode, C. Cardoza, H. K. A. Yasin, S. N. Mali, S. M. Tambe, P. Roy, K. Singh, A. D. Goel, P. Amin, B. R. Thorat, J. N. Cruz and A. P. Pratap, Green surfactants (biosurfactants): a petroleum-free substitute for sustainability-comparison, applications, market, and future prospects, *ACS Omega*, 2023, **13**, 11674–11699, DOI: 10.1021/acsomega.3c00591.

8 A. O. Mawlid, H. H. Abdelhady, M. G. Abd El-Moghny, A. Hamada, F. Abdelnaby, M. Kased, S. Al-Bajouri, R. A. Elbohy and M. S. El-Deab, Clean approach for catalytic biodiesel production from waste frying oil utilizing K2CO3/orange peel derived hydrochar via RSM Optimization, *J. Cleaner Prod.*, 2024, **442**, 140947, DOI: 10.1016/j.jclepro.2024.140947.

9 E. K. L. Mares, M. A. Gonçalves, P. T. S. Luz, G. N. R. Filho, J. R. Zamian and L. R. V. Conceição, Acai seed ash as a novel basic heterogeneous catalyst for biodiesel synthesis: optimization of the biodiesel production process, *Fuel*, 2021, **299**, 120887, DOI: 10.1016/j.fuel.2021.120887.

10 I. M. Mendonça, F. L. Machado, C. C. Silva, S. D. Junior, M. L. Takeno, P. J. S. Maia, L. Manzato and F. A. Freitas, Application of calcined waste cupuaçu (Theobroma grandiflorum) seeds as a low-cost solid catalyst in soybean oil ethanolysis: statistical optimization, *Energy Convers. Manage.*, 2019, **200**, 112095, DOI: 10.1016/j.enconman.2019.112095.

11 M. Yajun, J. Yaling, S. Xiangmin, L. Xiaogai, M. Jieyi and C. Shihong, Modified banana peel biochar-based green nanocatalyst for biodiesel production and its utilization to improve diesel engine performance and emission, *Process Saf. Environ. Prot.*, 2024, **191**, 1617–1632, DOI: 10.1016/j.psep.2024.09.009.

12 M. Basir, E. Hossein, K. Y. Venkatesh and E. Amruth, Valorization of dairy waste scum oil and rice husk ash-supported CuO nanocatalyst towards cleaner production of biodiesel: a waste-to-energy approach, *Process Saf. Environ. Prot.*, 2024, **192**, 1393–1407, DOI: 10.1016/j.psep.2024.10.124.

13 E. O. Babatunde, S. Enomah, O. M. Akwenuke, T. F. Adepoju, C. O. Okwelum, M. M. Mundu, A. Aiki and O. D. Oghenejabor, Novel-activated carbon from waste green coconut husks for the synthesis of biodiesel from pig fat oil blends with tallow seed oil, *Case Stud. Chem. Environ. Eng.*, 2025, **11**, 101058, DOI: 10.1016/j.cscee.2024.101058.

14 N. Daimary, K. S. H. Eldiehy, N. Bora, P. Boruah, M. A. Rather, M. Mandal, U. Bora and D. Deka, Towards integrated sustainable biofuel and chemical production: an application of banana pseudostem ash in the production of biodiesel and recovery of lignin from bamboo leaves, *Chemosphere*, 2023, **314**, 137625, DOI: 10.1016/j.chemosphere.2022.137625.

15 I. B. Laskar, R. Gupta, S. Chatterjee, C. Vanlalveni and S. L. Rokhum, Taming waste: waste Mangifera indica peel as a sustainable catalyst for biodiesel production at room temperature, *Renew. Energy*, 2020, **161**, 207–220, DOI: 10.1016/j.renene.2020.07.061.

16 B. Changmai, P. Sudarsanam and S. L. Rokhum, Biodiesel production using a renewable mesoporous solid catalyst, *Ind. Crops Prod.*, 2020, **145**, 111911, DOI: 10.1016/j.indcrop.2019.111911.

17 IBRAFE, Instituto Brasileiro de Feijão e Pulses, *Cenário brasileiro do Feijão-caupi*, https://www.ibrafe.org/artigo/cenario-brasileiro-do-feijao-caupi, 2022, acessed 27 October 2023.

18 Z. Kassab, Y. Abdellaoui, M. H. Salim and M. El Achaby, Cellulosic materials from pea (*Pisum Sativum*) and broad beans (*Vicia Faba*) pods agro-industrial residues, *Mater. Lett.*, 2020, **280**, 128539, DOI: 10.1016/j.matlet.2020.128539.

19 E. C. Emenike, H. K. Okoro, A. G. Adeniyi, K. O. Iwuozor, C. Zvinowanda and J. C. Ngila, Applications of bean pod and husk for remediation of water contamination: a review, *Bioresour. Technol. Rep.*, 2024, **25**, 101754, DOI: 10.1016/j.biteb.2023.101754.

20 O. S. Bello, O. C. Alao, T. C. Alagbada and A. M. Olatunde, Biosorption of ibuprofen using functionalized bean husks, *Sustainable Chem. Pharm.*, 2019, **13**, 100151, DOI: 10.1016/j.scp.2019.100151.

21 J. L. Aleman-Ramirez, P. U. Okoye, U. Pal and P. J. Sebastian, Agro-industrial residue of Pouteria sapota peels as a green heterogeneous catalyst to produce biodiesel from soybean and sunflower oils, *Renew. Energy*, 2024, **224**, 120163, DOI: 10.1016/j.renene.2024.120163.

22 H. P. Boehm, Some aspects of the surface chemistry of carbon blacks and other carbons, *Carbon*, 1994, **32**(5), 759–769, DOI: 10.1016/0008-6223(94)90031-0.

23 C. Silva, T. A. Weschenfelder, S. Rovani, F. C. Corazza, M. L. Corazza, C. Dariva, *et al.*, Continuous production of fatty acid ethyl esters from soybean oil in compressed ethanol, *Ind. Eng. Chem. Res.*, 2007, **46**, 5304–5309, DOI: 10.1021/ie070310r.

24 R. Foroutan, S. J. Peighambardoust, R. Mohammadi, S. H. Peighambardoust and B. Ramavandi, Application of walnut shell ash/ZnO/K2CO3 as a new composite catalyst for biodiesel generation from Moringa oleifera oil, *Fuel*, 2022, **311**, 122624, DOI: 10.1016/j.fuel.2021.122624.

25 M. Kumar, S. K. Shukla, S. N. Upadhyay and P. K. Mishra, Analysis of thermal degradation of banana (Musa balbisiana) trunk biomass waste using iso-conversional models, *Bioresour. Technol.*, 2020, **310**, 123393, DOI: 10.1016/j.biortech.2020.123393.

26 B. Behera, M. S. Selvam, B. Dey and P. Balasubramanian, Algal biodiesel production with engineered biochar as a heterogeneous solid acid catalyst, *Bioresour. Technol.*, 2020, **310**, 123392, DOI: 10.1016/j.biortech.2020.123392.

27 S. F. Basumatary, B. Das, S. Brahma and S. Basumatary, Musa ABB (Kachkal) banana waste derived heterogeneous nanocatalyst for transesterification of binary oil mixture of Jatropha curcas and Pongamia pinnata to biodiesel, *Bioresour. Technol. Rep.*, 2025, **29**, 102018, DOI: 10.1016/j.biteb.2024.102018.

28 R. Lima-Corrêa, C. Castro and J. Assaf, Lithium containing MgAl mixed oxides obtained from sol-gel hydrotalcite for transesterification, *Braz. J. Chem. Eng.*, 2018, **35**, 189–195, DOI: 10.1590/0104-6632.20180351s20160146.

29 M. R. Avhad and J. M. Marchetti, Innovation in solid heterogeneous catalysis for the generation of economically viable and ecofriendly biodiesel: a review, *Catal. Rev.*, 2016, **58**(2), 157–208, DOI: 10.1080/01614940.2015.1103594.

30 A. Dejean, I. W. K. Ouédraogo, S. Mouras, J. Valette and J. Blin, Shea nut shell based catalysts for the production of ethanolic biodiesel, *Energy Sustainable Dev.*, 2017, **40**, 103–111, DOI: 10.1016/j.esd.2017.07.006.

31 N. Viriya-empikul, P. Krasae, W. Nualpaeng, B. Yoosuk and K. Faungnawakij, Biodiesel production over Ca-based solid catalysts derived from industrial wastes, *Fuel*, 2012, **92**, 239–244, DOI: 10.1016/j.fuel.2011.07.013.

32 M. H. Husin, M. Riza, M. Faisal and A. Sulastri, Biodiesel production using waste banana peel as renewable base catalyst, *Mater. Today: Proc.*, 2023, **87**, 214–217, DOI: 10.1016/j.matpr.2023.02.400.

33 M. Balajii and S. Niju, A novel biobased heterogeneous catalyst derived from Musa acuminata peduncle for biodiesel production – process optimization using central composite design, *Energy Convers. Manage.*, 2019, **189**, 118–131, DOI: 10.1016/j.enconman.2019.03.085.

34 B. Basumatary, S. Brahma, B. Nath, S. F. Basumatary, B. Das and S. Basumatary, Post-harvest waste to value-added materials: Musa champa plant as renewable and highly effective base catalyst for Jatropha curcas oil-based biodiesel production, *Bioresour. Technol. Rep.*, 2023, **21**, 101338, DOI: 10.1016/j.biteb.2023.101338.

35 G. P. Chutia, S. Chutia, P. Kalita and K. Phukan, Xanthium strumarium seed as a potential source of heterogeneous catalyst and non-edible oil for biodiesel production, *Biomass Bioenergy*, 2023, **172**, 106773, DOI: 10.1016/j.biombioe.2023.106773.

36 V. Khiangte, S. Lalhmangaihzuala, Z. T. Laldinpuii, L. Nunnemi, R. B. Muthukumaran and K. Vanlaldinpuia, Novel dragon fruit peel ash-derived solid catalyst for biodiesel production and PET waste recycling, *Bioresour. Technol. Rep.*, 2023, **24**, 101663, DOI: 10.1016/j.biteb.2023.101663.

37 B. Nath, P. Kalita, B. Das and S. Basumatary, Highly efficient renewable heterogeneous base catalyst derived from waste Sesamum indicum plant for synthesis of biodiesel, *Renew. Energy*, 2020, **151**, 295–310, DOI: 10.1016/j.renene.2019.11.029.

38 M. R. Miladinović, M. V. Zdujić, D. N. Veljović, J. B. Krstić, I. B. Banković-Ilić, V. B. Veljković and O. S. Stamenković, Valorization of walnut shell ash as a catalyst for biodiesel production, *Renew. Energy*, 2020, **147**, 1033–1043, DOI: 10.1016/j.renene.2019.09.056.

39 G. P. Chutia and K. Phukan, Jute leaves ash@Fe3O4 as efficient nanocatalyst for sustainable biodiesel production: characterization, optimization and kinetic investigation, *J. Ind. Eng. Chem.*, 2024, **131**, 288–304, DOI: 10.1016/j.jiec.2023.10.028.

40 K. S. H. Eldiehy, M. Gohain, N. Daimary, D. Borah, M. Mandal and D. Deka, Radish (Raphanus sativus L.) leaves: a novel source for a highly efficient heterogeneous base catalyst for biodiesel production using waste soybean cooking oil and Scenedesmus obliquus oil, *Renew. Energy*, 2022, **191**, 888–901, DOI: 10.1016/j.renene.2022.04.070.

41 N. Daimary, K. S. H. Eldiehy, P. Boruah, D. Deka, U. Bora and B. K. Kakati, Potato peels as a sustainable source for biochar, bio-oil and a green heterogeneous catalyst for biodiesel production, *J. Environ. Chem. Eng.*, 2022, **10**, 107108, DOI: 10.1016/j.jece.2021.107108.

42 C. B. Ezekannagha, O. D. Onukwuli, I. A. Nnanwube, U. L. Ezeamaku and C. M. Ohaegbulam, Green hetero-alkali catalyst in optimized waste lard oil transesterification for biodiesel synthesis, *Results Chem.*, 2024, **11**, 101797, DOI: 10.1016/j.rechem.2024.101797.

43 E. A. Olatundun, O. O. Borokini and E. Betiku, Cocoa pod husk-plantain peel blend as a novel green heterogeneous catalyst for renewable and sustainable honne oil biodiesel synthesis: a case of biowastes-to-wealth, *Renew. Energy*, 2020, **166**, 163–175, DOI: 10.1016/j.renene.2020.11.131.

44 A. Mulkan, N. W. M. Zulkifli, H. Husin, Ahmadi, I. Dahlan and S. Syafiie, Development of jackfruit (Artocarpus heterophyllus) peel waste as a new solid catalyst: biodiesel synthesis, optimization and characterization, *Process Saf. Environ. Prot.*, 2023, **177**, 152–168, DOI: 10.1016/j.psep.2023.07.021.

45 B. Nath, B. Das, P. Kalita and S. Basumatary, Waste to value addition: utilization of waste Brassica nigra plant derived novel green heterogeneous base catalyst for effective synthesis of biodiesel, *J. Cleaner Prod.*, 2019, **239**, 118112, DOI: 10.1016/j.jclepro.2019.118112.

46 G. Pathak, D. Das, K. Rajkumari and L. Rokhum, Exploiting waste: towards a sustainable production of biodiesel using *Musa acuminata* peel ash as a heterogeneous catalyst, *Green Chem.*, 2018, **20**, 2365, DOI: 10.1039/C8GC00071A.

47 J. L. Aleman-Ramirez, J. Moreira, S. Torres-Arellano, A. Longoria, P. U. Okoye and P. J. Sebastian, Preparation of a heterogeneous catalyst from moringa leaves as a sustainable precursor for biodiesel production, *Fuel*, 2021, **284**, 118983, DOI: 10.1016/j.fuel.2020.118983.

48 B. Nath, B. Basumatary, S. Brahma, B. Das, P. Kalita, S. L. Rokhum and S. Basumatary, Musa champa peduncle waste-derived efficient catalyst: studies of biodiesel synthesis, reaction kinetics and thermodynamics, *Energy*, 2023, **270**, 126976, DOI: 10.1016/j.energy.2023.126976.

49 A. Sarkar, P. Das, I. B. Laskar, S. Vadivel, A. Puzari and B. Paul, Parkia speciosa: a basic heterogeneous catalyst for production of soybean oil-based biodiesel, *Fuel*, 2023, **348**, 128537, DOI: 10.1016/j.fuel.2023.128537.

50 P. Prajapati, S. Shrivastava, V. Sharma, P. Srivastava, V. Shankhwar, A. Sharma, S. K. Srivastava and D. D. Agarwal, Karanja seed shell ash: a sustainable green heterogeneous catalyst for biodiesel production, *Results Eng.*, 2023, **18**, 101063, DOI: 10.1016/j.rineng.2023.101063.

51 N. Ozbay, A. S. Yargic, R. Z. Y. Sahin and E. Yaman, Valorization of banana peel waste via in-situ catalytic pyrolysis using Al-modified SBA-15, *Renew. Energy*, 2019, **140**, 633–646, DOI: 10.1016/j.renene.2019.03.071.

52 B. Nath, B. Basumatary, N. Wary, U. Basumatary, J. Basumatary, S. L. Rokhum, M. Azam and K. Min, Basumatary agricultural waste-based heterogeneous catalyst for the production of biodiesel: a ranking study via the VIKOR method, *Int. J. Energy Res.*, 2023, **6**, 1–23, DOI: 10.1155/2023/7208754.

53 O. M. Akwenuke, C. O. Okwelum, T. A. Balogun, R. Nwadiolu, G. I. Okolotu, I. E. Chukwuma, T. F. Adepoju, A. E. Essaghah, A. F. Ibimilua and A. Taiga, Biodiesel production from agricultural biomass wastes: Duroc breed fat oil, Citrillus lanatus rind, and Sorghum Bagasse, *MethodsX*, 2024, **13**, 102948, DOI: 10.1016/j.mex.2024.102948.

54 A. Arumugam and P. Sankaranarayanan, Biodiesel production and parameter optimization: an approach to utilize residual ash from sugarcane leaf, a novel heterogeneous catalyst, from Calophyllum inophyllum oil, *Renew. Energy*, 2020, **153**, 1272–1282, DOI: 10.1016/j.renene.2020.02.101.

55 G. Pathak, K. Rajkumari and S. L. Rokhum, Wealth from waste: *M. acuminata* peel waste-derived magnetic nanoparticles as a solid catalyst for the Henry reaction, *Nanoscale Adv.*, 2019, **21**, 1013–1020, DOI: 10.1039/C8NA00321A.

56 B. R. Naidu and K. Venkateswarlu, Dried water extract of pomegranate peel ash (DWEPA) as novel and biorenewable heterogeneous catalyst for biodiesel production and biopotent quinoxalines synthesis, *Bioresour. Technol. Rep.*, 2022, **18**, 101107, DOI: 10.1016/j.biteb.2022.101107.

57 Y. Zhou, S. Niu and J. Li, Activity of the carbon-based heterogeneous acid catalyst derived from bamboo in esterification of oleic acid with ethanol, *Energy Convers. Manage.*, 2016, **14**, 188–196, DOI: 10.1016/j.enconman.2016.02.027.

58 H. H. Abdelhady, H. A. Elazab, E. M. Ewais, M. Saber and M. S. El-Deab, Efficient catalytic production of biodiesel using nano-sized sugar beet agro-industrial waste, *Fuel*, 2020, **261**, 116481, DOI: 10.1016/j.fuel.2019.116481.

59 B. Changmai, R. Rano, C. Vanlalveni and S. L. Rokhum, A novel Citrus sinensis peel ash coated magnetic nanoparticles as an easily recoverable solid catalyst for biodiesel production, *Fuel*, 2021, **286**, 119447, DOI: 10.1016/j.fuel.2020.119447.

60 M. Yuliana, S. P. Santoso, F. E. Soetaredjo, S. Ismadji, A. E. Angkawijaya, W. Irawaty, Y. Ju, P. L. Tran-Nguyen and S. B. Hartono, Utilization of waste capiz shell – based catalyst for the conversion of leather tanning waste into biodiesel, *J. Environ. Chem. Eng.*, 2020, **8**, 104012, DOI: 10.1016/j.jece.2020.104012.

61 Y. Lin, K. T. T. Amesho, C. C. Chen, P. C. Cheng and F. C. Chou, A cleaner process for green biodiesel synthesis from waste cooking oil using recycled waste oyster shells as a sustainable base heterogeneous catalyst under the microwave heating system, *Sustainable Chem. Pharm.*, 2020, **17**, 100310, DOI: 10.1016/j.scp.2020.100310.

62 S. Tamjidi, B. K. Moghadas and H. Esmaeili, Ultrasound-assisted biodiesel generation from waste edible oil using CoFe2O4@GO as a superior and reclaimable nanocatalyst: optimization of two-step transesterification by RSM, *Fuel*, 2022, **327**, 125170, DOI: 10.1016/j.fuel.2022.125170.

63 S. G. Khan, M. Hassan, M. Anwar, Z. Sheikh, U. M. Khan and C. Zhao, Mussel shell based CaO nano-catalyst doped with praseodymium to enhance biodiesel production from castor oil, *Fuel*, 2020, **330**, 125480, DOI: 10.1016/j.fuel.2022.125480.

64 J. Borah, H. J. Sarmah, N. Bhuyan, D. Mohanta and D. Deka, Application of Box Behnken design in optimization of biodiesel yield using WO 3/graphene quantum dot (GQD) system and its kinetics analysis, *Biomass Convers. Biorefin.*, 2020, **12**, 221–232, DOI: 10.1007/s13399-020-00717-x.

65 A. K. Rajak, H. Madiga, D. L. Mahato, R. Pothu, G. Periyasami, P. K. Sarangi, R. Boddula and K. S. L. Mallampalli, Exploring the peel ash of musa acuminate as a heterogeneous green catalyst for producing biodiesel from Niger oil: a sustainable and circular bio economic approach, *Sustainable Chem. Pharm.*, 2024, **39**, 101622, DOI: 10.1016/j.scp.2024.101622.

66 A. Das, H. Li, R. Kataki, P. S. Agrawal, N. S. Moyon, B. Gurunathan and S. L. Rokhum, Terminalia arjuna bark – a highly efficient renewable heterogeneous base catalyst for biodiesel production, *Renew. Energy*, 2023, **212**, 185–196, DOI: 10.1016/j.renene.2023.05.066.

67 D. Chaos-Hernández, H. E. Reynel-Avila, D. I. Mendoza-Castillo, A. Bonilla-Petriciolet and I. A. Aguayo-Villarreal, Functionalization and activation of carbon-based catalysts with KOH and calcium and their application in transesterification to produce biodiesel: optimization of catalytic properties and kinetic study, *Fuel*, 2022, **310**, 122066, DOI: 10.1016/j.fuel.2021.122066.

68 A. O. Etim, E. Betiku, S. O. Ajala, P. J. Olaniyi and T. V. Ojumu, Potential of Ripe Plantain Fruit Peels as an

Ecofriendly Catalyst for Biodiesel Synthesis: Optimization by Artificial Neural Network Integrated with Genetic Algorithm, *Sustainability*, 2018, **10**, 707, DOI: **10.3390/su10030707**.

69 C. Zhao, L. Pengmei, L. Yang, S. Xing, W. Luo and Z. Wang, Biodiesel synthesis over biochar-based catalyst from biomass waste pomelo peel, *Energy Convers. Manage.*, 2018, **160**, 477–485, DOI: **10.1016/j.enconman.2018.01.059**.

70 B. Basumatary, S. Basumatary, B. Das, B. Nath and P. Kalita, Waste Musa paradisiaca plant: an efficient heterogeneous base catalyst for fast production of biodiesel, *J. Cleaner Prod.*, 2021, **305**, 127089, DOI: **10.1016/j.jclepro.2021.127089**.

71 C. G. Lopresto, M. G. De Paola and V. Calabrò, Importance of the properties, collection, and storage of waste cooking oils to produce high-quality biodiesel – an overview, *Biomass Bioenergy*, 2024, **189**, 107363, DOI: **10.1016/j.biombioe.2024.107363**.

72 A. Al-Abbasi, F. Almahdi, M. Almaky, R. Izriq, A. Milad, S. Salim and A. Najar, BaO as a heterogeneous nanoparticle catalyst in oil transesterification for the production of FAME fuel, *Inorg. Chem. Commun.*, 2023, **158**, 111620, DOI: **10.1016/j.inoche.2023.111620**.

73 M. G. Basyouny, M. R. Abukhadra, K. Alkhaledi, A. M. El-Sherbeeny, M. A. El-Meligy, A. T. A. Soliman and M. Luqman, Insight into the catalytic transformation of the waste products of some edible oils (corn oil and palm oil) into biodiesel using MgO/clinoptilolite green nanocomposite, *Mol. Catal.*, 2021, **500**, 111340, DOI: **10.1016/j.mcat.2020.111340**.

74 K. Chana, B. Chen and D. Na-Ranong, Biodiesel produced from transesterification of palm oil using NaOH-treated activated carbon and pyrolytic char of used tires as catalysts, *Process Saf. Environ. Prot.*, 2025, **195**, 106750, DOI: **10.1016/j.psep.2025.01.004**.

75 M. Guo, W. Jiang, J. Ding and J. Lu, Highly active and recyclable CuO/ZnO as photocatalyst for transesterification of waste cooking oil to biodiesel and the kinetics, *Fuel*, 2022, **315**, 123254, DOI: **10.1016/j.fuel.2022.123254**.

76 G. Zhang, W. Liang, J. Liu, G. Chen, J. Yao, B. Yan, H. Wang and Y. Zhang, Sustainable biodiesel production from waste cooking oil using oyster shell-derived superparamagnetic acid-base bifunctional biochar, *Process Saf. Environ. Prot.*, 2025, **195**, 106820, DOI: **10.1016/j.psep.2025.106820**.

77 I. M. Mendonça, O. A. R. L. Paes, P. J. S. Maia, M. P. Souza, R. A. Almeida, C. C. Silva, S. Duvoisin and F. A. Freitas, New heterogeneous catalyst for biodiesel production from waste tucumã peels (Astrocaryum aculeatum Meyer): parameters optimization study, *Renew. Energy*, 2019, **130**, 103–110, DOI: **10.1016/j.renene.2018.06.059**.

78 T. S. Ribeiro, M. A. Gonçalves, G. N. R. Filho and L. R. V. Conceição, Functionalized Biochar from the Amazonian Residual Biomass Murici Seed: An Effective and Low-Cost Basic Heterogeneous Catalyst for Biodiesel Synthesis, *Molecules*, 2023, **28**, 7980, DOI: **10.3390/molecules28247980**.